

1 Examination of varying mixed-phase stratocumulus clouds in terms of their
 2 properties, ice processes and aerosol-cloud interactions between polar and
 3 midlatitude cases: An attempt to propose a microphysical factor to explain the
 4 variation

5

6 Seoung Soo Lee^{1,2,3}, Chang-Hoon Jung⁴, ~~Jinho Choi⁵~~, Young Jun Yoon⁶, Junshik Um^{5,7},
 7 Youtong Zheng⁸, Jianping Guo⁹, Manguttathil. G. Manoj¹⁰, Sang-Keun Song¹¹

8

9 ¹Science and Technology Corporation, Hampton, Virginia

10 ²Earth System Science Interdisciplinary Center, University of Maryland, College Park,
 11 Maryland, USA

12 ³Research Center for Climate Sciences, Pusan National University, Busan, Republic of
 13 Korea

14 ⁴Department of Health Management, Kyungin Women's University, Incheon, Republic of
 15 Korea

16 ~~⁵Department of Atmospheric Sciences, Pusan National University, Busan, Republic of~~
 17 ~~Korea~~

18 ~~⁶Korea Polar Research Institute, Incheon, Republic of Korea~~

19 ~~⁷Institute of Environmental Studies, Pusan National University, Busan, Republic of Korea~~

20 ⁸Department of Earth and Atmospheric Sciences, University of Houston, Houston, Texas,
 21 USA

22 ⁹State Key Laboratory of Severe Weather, Chinese Academy of Meteorological Sciences,
 23 Beijing 100081, China

Deleted: ⁵,Deleted: ⁶

Moved (insertion) [1]

Deleted: ⁶Deleted: a⁶Deleted: ⁵Moved up [1]: ⁶Department of Atmospheric Sciences, Pusan National University, Busan, Republic of Korea⁶

31 ¹⁰Advanced Centre for Atmospheric Radar Research, Cochin University of Science and
32 Technology, Kerala, India

33 ¹¹Department of Earth and Marine Sciences, Jeju National University, Jeju, Republic of
34 Korea

35

36

37

38

39

40

41

42

43

44

45

46

47

48

49

50

51

52

53

54

55 Corresponding author: Seoung Soo Lee, [Chang-Hoon Jung and Sang-Keun Song](#)

56 Office: (303) 497-6615

57 Cell: (609) 375-6685

58 Fax: (303) 497-5318

59 E-mail: cumulss@gmail.com, slee1247@umd.edu

60 **Abstract**

61

62 This study examines the ratio of ice crystal number concentration (ICNC) to cloud droplet
 63 number concentration (CDNC), which is ICNC/CDNC, in mixed-phase stratocumulus
 64 clouds. This examination is performed using a large-eddy simulation (LES) framework and
 65 one of efforts toward a more general understanding of mechanisms controlling cloud,
 66 development, aerosol-cloud interactions and impacts of ice processes on them in mixed-
 67 phase stratocumulus clouds. For the examination, this study compares a case of polar
 68 mixed-phase stratocumulus clouds to that of midlatitude mixed-phase stratocumulus
 69 clouds with weak precipitation. It is found that ICNC/CDNC plays a critical role in making
 70 differences in cloud development with respect to the relative proportion of liquid and ice
 71 mass between the cases by affecting in-cloud latent-heat processes. Note that this
 72 proportion has an important implication for cloud radiative properties and thus climate. It
 73 is also found that ICNC/CDNC plays a critical role in making differences in interactions
 74 between clouds and aerosols and impacts of ice processes on clouds and their interactions
 75 with aerosols, between the cases by affecting in-cloud latent-heat processes. Findings of
 76 this study suggest that ICNC/CDNC can be a simplified general factor that contributes to
 77 a more general understanding of mixed-phase clouds, their interactions with aerosols and
 78 roles of ice processes in them and thus, to the development of more general
 79 parameterizations of those clouds, interactions and roles.

80

81

82

83

84

85

86

87

88

89

90

Deleted: ,**Deleted:** as a microphysical factor that induces differences in cloud development, its interactions with aerosols and impacts of ice processes on them among cases of mixed-phase clouds.**Deleted:** those**Deleted:** phase**Deleted:** clouds and their**Deleted:** with**Deleted:** them**Deleted:** and aerosols

1. Introduction

101
102

103 Stratiform clouds (e.g., stratus and stratocumulus clouds) have significant impacts on
104 climate (Warren et al. 1986; Stephens and Greenwald 1991; Hartmann et al. 1992; Hahn
105 and Warren 2007; Wood, 2012; Dione et al., 2019; Zheng et al., 2021). Since
106 industrialization, aerosol concentrations have increased and this has had impacts on
107 stratiform clouds and climate (Twomey, 1974; Albrecht, 1989; [Ackerman et al., 2004](#)).
108 However, our level of understanding of these clouds and impacts has been low and this has
109 caused the highest uncertainty in the prediction of future climate (Ramaswamy et al., 2001;
110 Forster et al., 2007; Knippertz et al., 2011; Hannak et al., 2017). Stratiform clouds can be
111 classified into warm and mixed-phase clouds. Mixed-phase clouds involve ice processes
112 and frequently form in midlatitude and polar regions. Most previous studies have focused
113 on warm clouds and their interactions with aerosols, whereas the mixed-phase clouds and
114 their interactions with aerosols are poorly understood mainly due to the more complex ice
115 processes. Hence, mixed-phase clouds and their interactions with aerosols account for the
116 uncertainty more than warm clouds and their interactions with aerosols (Ramaswamy et al.,
117 2001; Forster et al., 2007; Wood, 2012; IPCC, 2021; Li et al., 2022).

118 The relative proportion of liquid mass, which can be represented by liquid-water
119 content (LWC) or liquid-water path (LWP), and ice mass, which can be represented by ice-
120 water content (IWC) or ice-water path (IWP), in mixed-phase stratiform clouds plays a
121 critical role in cloud radiative properties and thus their climate feedbacks (Choi et al., 2010
122 and 2014; [Zhang et al., 2019](#)). This is because radiative properties of liquid particles are
123 substantially different from those of ice particles. The relative proportion is defined to be
124 IWC (IWP) over LWC (LWP) or IWC/LWC (IWP/LWP) in this study. Motivated by this
125 and the above-mentioned uncertainty, this study aims to improve our understanding of
126 mixed-phase stratiform clouds and their interactions with aerosols with the emphasis on
127 ice processes and IWC/LWC (or IWP/LWP).

128 Lee et al. (2022) have investigated mixed-phase stratocumulus clouds in a midlatitude
129 region and found that microphysical latent-heat processes are more important in the
130 development of mixed-phase clouds and their interactions with aerosols than entrainment
131 and sedimentation processes. Lee et al. (2022) have found that a microphysical factor, the

Deleted: It is well-known that

Deleted: s

Deleted: there have been increases in

Deleted: It is known that

Deleted: t

137 ratio of ice crystal number concentration (ICNC) to cloud droplet number concentration
 138 (CDNC) or ICNC/CDNC, play an important role in latent processes, the development of
 139 mixed-phase clouds and their interactions with aerosols. In particular, Lee et al. (2022)
 140 have found that IWC/LWC or IWP/LWP is strongly affected by ICNC/CDNC. This is
 141 because deposition (condensation) of water vapor occurs on the surface of ice crystals
 142 (droplets). Thus, ice crystals (droplets) act as sources of deposition (condensation) and then
 143 IWC or IWP (LWC or LWP). More ice crystals (droplets) provide the greater integrated
 144 surface area of ice crystals (droplets) and induce more deposition (condensation) for a
 145 given environmental condition (Lee et al., 2009; Khain et al., 2012; Fan et al., 2018; Chua
 146 and Ming, 2020; Lee et al., 2022). Note that deposition and condensation are processes
 147 through which water vapor is removed, hence ice crystals and droplets are sinks of water
 148 vapor when deposition and condensation occur. However, when it comes to deposition and
 149 condensation themselves as microphysical processes, ice crystals (droplets) can be
 150 considered the sources of deposition and condensation. The higher ICNC/CDNC means
 151 more ice crystals or sources of deposition per a droplet as a source of condensation in a
 152 given group of ice crystals and droplets. Thus, the higher ICNC/CDNC enables more
 153 deposition per unit condensation to occur, which can raise IWC/LWC or IWP/LWP.

154 Mixed-phase stratocumulus clouds in different regions are known to have different
 155 IWC/LWC or IWP/LWP and aerosol-cloud interactions (e.g., Choi et al., 2010 and 2014;
 156 Zhang et al., 2019). Lots of factors such as environmental conditions, which can be
 157 represented by variables such as temperature, humidity and wind shear, can explain those
 158 differences. Choi et al. (2010 and 2014) and Zhang et al. (2019) have shown that as
 159 temperature lowers, IWC/LWC or IWP/LWP tends to increase and indicated that
 160 temperature is a primary environmental condition to explain the differences in IWC/LWC
 161 among different regions or clouds. However, Choi et al. (2010 and 2014) and Zhang et al.
 162 (2019) have not discussed process-level mechanisms that govern the role of temperature in
 163 those differences.

164 It is important to establish a general principle that explains the differences in
 165 LWC/LWC and aerosol-cloud interactions among regions, since the general principle is
 166 useful in the development of a more general or comprehensive parameterization of
 167 stratocumulus clouds and their interactions with aerosols for climate models. This

Deleted: they

Deleted: stability

Deleted: .

171 contributes to the better prediction of future climate, considering that the absence of the
 172 comprehensive parameterization has been considered one of the biggest obstacles to the
 173 better prediction (Ramaswamy et al., 2001; Foster et al., 2007; Stevens and Feingold, 2009).

174 As a way of contributing to the establishment of the general principle, this study
 175 attempts to take ICNC/CDNC as a general factor, which can constitute the general principle,
 176 to explain the differences in IWC/LWC (or IWP/LWP) and aerosol-cloud interactions
 177 among clouds. This study also attempts to elucidate ~~how~~ ice processes differentiate mixed-

Deleted: how

178 phase clouds from warm clouds in terms of cloud development and its interactions with
 179 aerosols, and how this differentiation varies among cases of mixed-phase clouds with

180 different ICNC/CDNC values. This attempt is valuable, considering that ~~in general,~~ the
 181 establishment of the general principle for stratocumulus clouds ~~and their interactions with~~

Deleted: t is generally accepted that

182 aerosols has been progressed much less than that for other types of clouds such as
 183 convective clouds ~~and their interactions with aerosols~~. The attempt is valuable, also

184 considering that our level of understanding of how ice processes differentiate mixed-phase
 185 clouds and their interactions with aerosols from much-studied warm clouds and their

186 interactions with aerosols has been low. ~~Here, we want to emphasize that this study does~~
 187 ~~not aim to gain a fully established general principle, but aims to test the factor that can be~~

188 ~~useful to move ahead on our path to a more complete general principle. Hence, this study~~
 189 ~~should be regarded a steppingstone to the established principle, and should not be~~

190 ~~considered a perfect study that get us the fully established principle. Taking into account~~
 191 ~~the fact that even attempts to provide general factors for the general principle have been~~

192 ~~rare, the fulfilment of the aim is likely to provide us with valuable preliminary information~~
 193 ~~that streamlines the development of a more established general principle.~~

194 For the attempt, this study investigates a case of mixed-phase, stratiform clouds in the
 195 polar region. Via the investigation, this study aims to identify process-level mechanisms

Deleted: ,

Deleted: d

196 that control the development of those clouds and their interactions with aerosols, and the
 197 impact of ice processes on the development and interactions using a large-eddy simulation

198 (LES) framework. Then, this study compares the mechanisms in the case of polar clouds
 199 to those in a case of midlatitude clouds which have been examined by Lee et al. (2022).

200 This comparison is based on Choi et al. (2010 and 2014) and Zhang et al. (2019) which
 201 have shown that temperature is an important factor which explains the differences in

206 IWC/LWC among regions or clouds. Due to significant differences in latitudes, noticeable
 207 differences in the temperature of air are between the polar and midlatitude cases. Hence,
 208 through this comparison, this study looks at the role of temperature in those differences in
 209 IWC/LWC and associated aerosol-cloud interactions. More importantly than that, as a way
 210 of identifying process-level mechanisms that control the role of temperature, this study
 211 tests how ICNC/CDNC as the general factor is linked to the role of temperature, using the
 212 LES framework. Through this test, this study also identifies process-level mechanisms that
 213 control how ICNC/CDNC affects roles of ice processes in the differentiation between
 214 mixed-phase and warm clouds in terms of cloud development and its interactions with
 215 aerosols, and causes the variation of the differentiation between the cases of mixed-phase
 216 stratiform clouds.

217 2. Case, model and simulations

218 2.1 LES model

219
 220
 221
 222 LES simulations are performed by using the Advanced Research Weather Research and
 223 Forecasting (ARW) model. A bin scheme, which is detailed in Khain et al. (2000) and
 224 Khain et al. (2011), is adopted by the ARW for the simulation of microphysics. Size
 225 distribution functions for each class of hydrometeors, which are classified into water drops,
 226 ice crystals (plate, columnar and branch types), snow aggregates, graupel and hail, and
 227 aerosols acting as cloud condensation nuclei (CCN) and ice-nucleating particles (INP) are
 228 represented with 33 mass doubling bins, i.e., the mass of a particle m_k in the k th bin is
 229 determined as $m_k = 2m_{k-1}$. Each of hydrometeors has its own terminal velocity that varies
 230 with the hydrometeor mass and the sedimentation of hydrometeors is simulated using their
 231 terminal velocity. The evolution of aerosol size distribution at each grid point is controlled
 232 by aerosol sinks and sources such as aerosol advection, turbulent mixing and activation. It
 233 is assumed that aerosols do not fall down by themselves and move around by airflow that
 234 is composed of horizontal flow, updrafts, downdrafts and turbulent motions. When aerosols
 235 move with airflow, it is assumed that they move with the same velocity as airflow. Taking
 236 activation as an example of the evolution of aerosol size distribution, the bins of the aerosol

Deleted: T

Deleted: s

Deleted: a

Deleted: , which contributes to the establishment of the general principle...

Deleted: , to explain the differences in IWC/LWC (or IWP/LWP) and aerosol-cloud interactions among cases of mixed-phased stratiform clouds.

Deleted: comparison

Deleted: contributes to

Deleted: different

Deleted: among

Deleted: 2.1

Formatted: Font: Bold

Formatted: Outline numbered + Level: 2 + Numbering Style: 1, 2, 3, ... + Start at: 1 + Alignment: Left + Aligned at: 0.5" + Indent at: 0.75"

250 spectra that correspond to activated particles are emptied. Activated aerosol particles are
 251 included in hydrometeors and move to different classes and sizes of hydrometeors through
 252 collision-coalescence. In case hydrometeors with aerosol particles precipitate to the surface,
 253 those particles are removed from the atmosphere.

254 The large energetic turbulent eddies are directly resolved by the LES framework, and
 255 the effects of the smaller subgrid-scale turbulent motions on the resolved flow are
 256 parameterized based on the most widely used method that Smagorinsky (1963) and Lilly
 257 (1967) proposed. In this method, the mixing time scale is defined to be the norm of the
 258 strain rate tensor (Bartosiewicz and Duponcheel, 2018). A cloud-droplet nucleation
 259 parameterization based on Köhler theory represents cloud-droplet nucleation. Arbitrary
 260 aerosol mixing states and aerosol size distributions can be fed to this parameterization. To
 261 represent heterogeneous ice-crystal nucleation, the parameterizations by Lohmann and
 262 Diehl (2006) and Möhler et al. (2006) are used. In these parameterizations, contact,
 263 immersion, condensation-freezing, and deposition nucleation paths are all considered by
 264 taking into account the size distribution of INP, temperature and supersaturation.
 265 Homogeneous aerosol (or haze particle) and droplet freezing is
 266 also considered following the theory developed by Koop et al. (2000).

267 The bin microphysics scheme is coupled to the Rapid Radiation Transfer Model
 268 (RRTM; Mlawer et al., 1997). The effective sizes of hydrometeors, which are calculated
 269 in the bin scheme, are fed into the RRTM as a way of considering effects of the effective
 270 sizes on radiation. The surface process and resultant surface heat fluxes are simulated by
 271 the interactive Noah land surface model (Chen and Dudhia, 2001).

272

273 2.2 Case and simulations

274

275 2.2.1 Case and standard simulations

276

277 In the Svalbard area, Norway, a system of mixed-phase stratocumulus clouds existed over
 278 the horizontal domain marked by a red rectangle in Figure 1 and a period between ~02:00
 279 local solar time (LST) and 10:00 LST on March 29th, 2017. These clouds are observed by
 280 ground radar and lidar and these radar and lidar are a part of the Cloudnet ground

Deleted: was proposed by

Deleted: was observed to

Deleted: 2

284 observation that is deployed at a location in the red rectangle. The Cloudnet ground
 285 observation is composed of a suite of instruments such as lidar, radar and radiometer and
 286 described in Hogan et al. (2006). On average, the bottom and top of these clouds are at
 287 ~400 m and ~3 km in altitude, respectively, according to observation by those radar and
 288 lidar. The simulation of the observed system or case, i.e., the control run, is performed
 289 three-dimensionally over the red rectangle and the period. The horizontal domain adopts
 290 a 100-m resolution for the control run. The length of the domain in the horizontal directions
 291 is 50 km. The length of the domain in the vertical direction is ~5 km and the resolution for
 292 the vertical domain gets coarsened with height from ~20 m just above the surface to ~100
 293 m at the model top. Reanalysis data, which are produced by Met Office Unified Model
 294 (Brown et al., 2012) every 6 hours on a $0.11^\circ \times 0.11^\circ$ grid, provide potential temperature,
 295 specific humidity, and wind as initial and boundary conditions, which represent synoptic-
 296 scale environment, for the control run. The control run employs an open lateral boundary
 297 condition. Figure 2a shows the vertical distribution of the domain-averaged potential
 298 temperature and humidity in those reanalysis data at the first time step. A neutral, mixed
 299 layer is between the surface and 1 km in altitude as an initial condition (Figure 2a). Figure
 300 2b shows the time evolution of the domain-averaged large-scale subsidence or downdraft
 301 in the reanalysis data and at the model top. The large-scale subsidence gradually reduces
 302 with time (Figure 2b). Figure 2c shows the time evolution of the domain-averaged surface
 303 temperature in the reanalysis data. This evolution of the surface temperature is mostly
 304 controlled by the sea surface temperature (SST) considering that most portion of the red-
 305 rectangle domain is accounted for by the ocean (Figure 1). Between ~06:00 LST around
 306 when the sun rises and ~08:00 LST, the surface temperature increases from -2.2 to -1.6 °C,
 307 and after that, it does not show significant increase or decrease (Figure 2c).

308 The properties of cloud condensation nuclei (CCN) such as the number concentration,
 309 size distribution and composition are measured in the domain (Tunved et al., 2013; Jung et
 310 al., 2018). The measurement indicates that on average, aerosol particles are an internal
 311 mixture of 70 % ammonium sulfate and 30 % organic compound. This mixture is assumed
 312 to represent aerosol chemical composition over the whole domain and simulation period
 313 for this study. The observed and averaged concentration of aerosols acting as CCN is ~200
 314 cm^{-3} over the simulation period. Based on this, 200 cm^{-3} as an averaged concentration of

Deleted:

Deleted: .

Deleted:

Deleted: for the period on a three-dimensional domain of which horizontal extent is marked by a red rectangle in Figure 1.

Deleted: A

Deleted: is adopted by the horizontal domain in

Deleted: P

Deleted: .

Deleted: are provided by reanalysis data that are produced by Met Office Unified Model (Brown et al., 2012) every 6 hours on a $0.11^\circ \times 0.11^\circ$ grid

Deleted: There is

Deleted: a

Formatted: Font: (Asian) Batang

Deleted: There is a ground station in the domain (Tunved et al., 2013; Jung et al., 2018). This station measures

Deleted: t

Deleted: .

Deleted: by the station

334 aerosols acting as CCN is interpolated into all of grid points immediately above the surface
335 at the first time step.

336 ~~This study does not take into account~~ aerosol effects on radiation before aerosol is
337 activated, ~~since no significant amount of radiation absorbers is found~~ in the mixture. Based
338 on observation, the size distribution of aerosols acting as CCN is assumed to be a tri-modal
339 log-normal distribution (Figure 3). The shape of distribution, which is a tri-modal log-
340 normal distribution, as shown in Figure 3 is applied to the size distribution of aerosols
341 acting as CCN in all parts of the domain during the whole simulation period. The assumed
342 shape in Figure 3 is obtained by performing the average on the size distribution parameters
343 (i.e., modal radius and standard deviation of each of nuclei, accumulation and coarse modes,
344 and the partition of aerosol number among those modes) over the simulation period. ~~This~~
345 ~~study takes an assumption~~ that the interpolated CCN concentrations do not vary with height
346 in a layer between the surface and the planetary boundary layer (PBL) top around 1 km in
347 altitude. However, above the PBL top, ~~they are assumed to~~ decrease exponentially with
348 height, although the shape of size distribution and composition do not change with height.
349 It is assumed that ~~the properties of INP and CCN are not different~~ except for concentrations.
350 ~~The concentration of aerosols acting as CCN is assumed to be~~ 100 times higher than that
351 acting as INP over grid points at the first time step based on a general difference in
352 concentrations between CCN and INP (Pruppacher and Klett, 1978). Hence, the
353 concentration of aerosols acting as INP at the first time step is 2 cm^{-3} in the control run.
354 This assumed concentration of aerosols acting as INP is higher than usual (Seinfeld and
355 Pandis, 1998). However, Hartmann et al. (2021) observed the INP concentration that was
356 higher than assumed here in the Svalbard area when ~~strong dust events occur~~, meaning that
357 the assumed INP concentration is not that unrealistic.

358 To examine effects of aerosols on mixed-phase clouds, the control run is repeated by
359 increasing the concentration of aerosols by a factor of 10. In the repeated (control) run, the
360 initial concentrations of aerosols acting as CCN and INP at grid points immediately above
361 the surface are 2000 (200) and $20 (2) \text{ cm}^{-3}$, respectively. Reflecting these concentrations in
362 the simulation name, the control run is referred to as “the 200_2 run” and the repeated run
363 is referred to as “the 2000_20 run”. To isolate effects of aerosols acting as CCN (INP) on
364 mixed-phase clouds, the control run is repeated again by increasing the concentration of

Deleted: A

Deleted: are not taken into account for this study

Deleted: there is

Deleted: It is

Deleted: ed

Deleted: it is assumed that

Deleted: there are no differences in

Deleted: It is also assumed that

Deleted: t

Deleted: there were

375 aerosols acting as CCN (INP) only but not INP (CCN) by a factor of 10. In this repeated
376 run with the increase in the concentration of aerosols acting as CCN (INP), the initial
377 concentrations of aerosols acting as CCN and IFN at grid points immediately above the
378 surface are 2000 (200) and 2 (20) cm^{-3} , respectively. Reflecting this, the repeated run is
379 referred to as “the 2000_2 (200_20) run”.

380

381 2.2.2 Additional simulations

382

383 To isolate impacts of ice processes on the adopted case and its interactions with aerosols,
384 the 200_2 and 2000_2 runs are repeated by removing ice processes. These repeated runs
385 are referred to as the 200_2_noice and 2000_2_noice runs. In the 200_2_noice and
386 2000_2_noice runs, all hydrometeors (i.e., ice crystals, snow, graupel, and hail), phase
387 transitions (e.g., deposition and sublimation) and aerosols (i.e., INP) which are associated
388 with ice processes are removed. Hence, in these runs, only droplets (i.e., cloud liquid),
389 raindrops, associated phase transitions (e.g., condensation and evaporation) and aerosols
390 acting as CCN are present, regardless of temperature. Stated differently, these noice runs
391 simulate the warm-cloud counterpart of the selected mixed-phase cloud system. Via
392 comparisons between a pair of the 200_2 and 2000_2 runs and a pair of the 200_2_noice
393 and 2000_2_noice runs, the role of ice processes in the differentiation between mixed-
394 phase and warm clouds is to be identified. Along with this identification, the role of the
395 interplay between ice crystals and droplets in the development of the selected mixed-phase
396 cloud system and its interactions with aerosols is to be isolated.

397 As detailed in Sections 3.1.2 and 3.2.2 below, the test of ICNC/CDNC as a general
398 factor requires more simulations to see impacts of ICNCavg/CDCNavg on clouds and their
399 interactions with aerosols. Here, ICNCavg (CDNCavg) represents the average ICNC
400 (CDNC) over grid points and time steps with non-zero ICNC (CDNC).
401 ICNCavg/CDNCavg represents overall ICNC/CDNC over the domain and simulation
402 period. To respond to this requirement, 200_2_fac10, 200_2_fac10_CCN10,
403 200_2_fac10_INP10 runs are performed and their details are given in Sections 3.1.2 and
404 3.2.2. In addition, all the simulations above are repeated by turning off radiative processes
405 and Section 3.3 provides the details of these repeated simulations. These repeated runs are

Deleted:

407 the 200_2_norad, 2000_20_norad, 2000_2_norad, 200_20_norad, 200_2_noice_norad,
 408 2000_2_noice_norad, 200_2_fac10_norad, 200_2_fac10_CCN10_norad and
 409 200_2_fac10_INP10_norad runs. Moreover, based on the argument in Section 4.2, the
 410 4000_45, 13_0.1, 4000_1.8_fac10 and 12_0.0035_fac10 runs are performed and details of
 411 these runs are provided in Section 4.2. The summary of simulations in this study is given
 412 in Table 1.

413

414 3. Results

415

416 3.1 The 200_2 run vs. the 200_2_noice run

417

418 This study adopts the Cloudnet ground observation to evaluate the 200_2 run. Observed
 419 LWP is provided by radiometer. The retrieval of IWP is performed by using radar
 420 reflectivity and lidar backscatter as described in Donovan et al. (2001), Donovan (2003)
 421 and Tinel et al. (2005). As mentioned above, observed cloud-bottom and -top heights are
 422 obtained from radar and lidar measurements. Simulated LWP and IWP, as shown in Figure
 423 4 and Table 2, are compared to the observed LWP and retrieved IWP, respectively. The
 424 average LWP over all time steps and grid columns is 1.23 in the 200_2 run and 1.12 in
 425 observation. The average IWP over all time steps and grid columns is 31.94 in the 200_2
 426 run and 29.10 in retrieval. Cloud-bottom height, which is averaged over grid columns and
 427 time steps with non-zero cloud-bottom height, is 420 and 440 m in the 200_2 run and
 428 observation, respectively. Cloud-top height, which is averaged over grid columns and time
 429 steps with non-zero cloud-top height, is 3.5 and 3.3 km in the 200_2 run and observation,
 430 respectively. Each of LWP, cloud-bottom and -top heights shows an ~10% difference
 431 between the 200_2 run and observation. IWP also shows an ~10% difference between the
 432 200_2 run and retrieval. Thus, the 200_2 run is considered performed reasonably well for
 433 these variables.

434 To provide additional or supplementary information of cloud development, the time
 435 evolution of the simulated and observed cloud-top height is shown together with the
 436 simulated evolution of the surface sensible and latent-heat fluxes in Supplementary Figure
 437 1. This is based on the fact that the cloud-top height is considered a good indicative of

Formatted: Indent: Left: 0.75", No bullets or numbering

Deleted: ¶

Deleted:

Formatted: Font: Not Italic

Formatted: Font: Not Italic

Formatted: Font: Not Italic

Formatted: Font: Not Italic

Formatted: Font: Not Italic

Formatted: Font: Not Italic

Formatted: Font: Not Italic

Formatted: Font: Not Italic

440 cloud development and the surface fluxes are considered important parameters controlling
 441 the overall development of clouds. Simulated evolutions in Supplementary Figure 1 are
 442 from the 200_2 run. The cloud-top height increases between 02:00 and ~05:00 LST and
 443 after ~05:00 LST, it reduces gradually. The surface fluxes reduce with time, although the
 444 reduction rate of the fluxes starts to decrease around 08:00 LST in association with the
 445 increase in the surface temperature between ~06:00 and ~08:00 LST as shown in Figure
 446 2c.

447 The time- and domain-averaged IWP (IWC) is ~one order of magnitude greater than
 448 LWP (LWC) in the 200_2 run (Figure 4 and Table 2). For the sake of simplicity, the
 449 averaged IWC (IWP) over the averaged LWC (LWP) is denoted by IWC (IWP)/LWC
 450 (LWP), henceforth. IWC/LWC and IWP/LWP are 26.28 and 25.96, respectively, in the
 451 200_2 run. Since IWP and LWP are vertically integrated IWC and LWC over the vertical
 452 domain, respectively, the qualitative nature of differences between IWC and LWC is not
 453 much different from that between IWP and LWP. Hence, mentioning both a pair of IWC
 454 and LWC and that of IWP and LWP is considered redundant, and mentioning either a pair
 455 of IWC and LWC or that of IWP and LWP enhances the readability. Henceforth, IWC and
 456 LWC are chosen to be mentioned in text, although all of IWC, LWC, IWP and LWP are
 457 displayed in Tables 2 and 3.

458 Choi et al. (2014) and Zhang et al. (2019) have obtained the supercooled cloud fraction
 459 (SCF), which is basically the ratio of LWC to the sum of LWC and IWC and denoted by
 460 LWC/(LWC+IWC), using satellite- and ground-observed data collected over the period of
 461 ~5 years and ~1 year, respectively. Choi et al. (2014) have shown that SCF is as low as
 462 ~0.01 for the temperature range between -16 and -33 °C. Zhang et al. (2019) have also
 463 shown that SCF is as low as ~0.03 for the same temperature range, although the occurrence
 464 of SCF of ~0.03 or lower is rare. Note that the average air temperature immediately below
 465 the cloud base and above the cloud top over the simulation period is -16 and -33 °C,
 466 respectively, in the 200_2 run, and SCF in the 200_2 run is 0.04. Hence, based on Choi et
 467 al. (2014) and Zhang et al. (2019), we believe that SCF in the 200_2 run is observable and
 468 thus not that unrealistic, although it may not occur frequently.

469 To understand process-level mechanisms that control the results, microphysical
 470 processes are analyzed. As indicated by Ovchinnikov et al. (2011), in clouds with weak

Deleted:

Formatted: Font: (Default) Times New Roman, (Asian) Malgun Gothic, 12 pt, Font color: Auto

Deleted:

473 precipitation, a high-degree correlation is found between JWC and deposition or between
 474 LWC and condensation, considering that deposition and condensation are sources of JWC
 475 and LWC , respectively. In the 200_2 run, the average surface precipitation rate over the
 476 simulation period is $\sim 0.0020 \text{ mm hr}^{-1}$, which can be considered weak. Hence, in this case,
 477 condensation and deposition are considered proxies for JWC and LWC , respectively. Based
 478 on this, to gain a process-level understanding of microphysical processes that control the
 479 simulated JWC and LWC , condensation and deposition are analyzed.

Deleted: there is ... high-degree correlation is found between IWC (IWP...WC)...and deposition or between LWC (...WP...C)...and condensation, considering that deposition and condensation are sources of IWC (IWP...WC)...and LWC (...WP...C)... respectively. In the 200_2 run, the average surface precipitation rate over the simulation period is $\sim 0.0020 \text{ mm hr}^{-1}$, which can be considered weak. Hence, in this case, condensation and deposition are considered proxies for IWC (IWP...WC)...and LWC (...WP...C)... respectively. Based on this, to gain a process-level understanding of microphysical processes that control the simulated IWC (IWP...WC)...and...LWC (...WP...C) ... [1]

480 As seen in Figure 5 and Table 2, the average deposition rate is \sim one order of magnitude
 481 greater than condensation rate in the 200_2 run, leading to much greater JWC than LWC
 482 in the 200_2 run. This is in contrast to the situation in the case of mixed-phase
 483 stratocumulus clouds, which were located in a midlatitude region, in Lee et al. (2022). In
 484 this case, the average JWC and LWC are at the same order of magnitude. For the sake of
 485 brevity, this case in Lee et al. (2022) is referred to as “the midlatitude case”, while the case
 486 of mixed-phase clouds, which is adopted by this study, in the Svalbard area is referred to
 487 “the polar case”, henceforth. In the midlatitude case, JWC/LWC is ~ 1.55 , which is \sim one
 488 order of magnitude smaller than that in the polar case.

Deleted: IWC (IWP...WC)...than LWC (...WP...C)...in the 200_2 run. This is in contrast to the situation in the case of mixed-phase stratocumulus clouds, which were located in a midlatitude region, in Lee et al. (2022). In this case, the average IWC (IWP...WCP)...and LWC (...WP...C)...are at the same order of magnitude. For the sake of brevity, this case in Lee et al. (2022) is referred to as “the midlatitude case”, while the case of mixed-phase clouds, which is adopted by this study, in the Svalbard area is referred to “the polar case”, henceforth. In the midlatitude case, IWC/LWC and IWP...WC/LWP...C isare...1.55 and ...557... respectively, ...which isare...one order of magnitude smaller than thase... [2]

489 Warm clouds in the 200_2_noice run shows that the time- and domain-averaged
 490 condensation rate that is lower than the time- and the domain-averaged sum of
 491 condensation and deposition rates in the 200_2 run (Figure 5 and Table 2). This leads to a
 492 situation where warm clouds in the 200_2_noice run shows the time- and domain-averaged
 493 LWC that is lower than the time- and domain-averaged water content (WC), which is the
 494 sum of JWC and LWC , in mixed-phase clouds in the 200_2 run (Figure 4 and Table 2).
 495 This is despite the fact that LWC in the 200_2_noice run is higher than JWC in the 200_2
 496 run (Figure 4 and Table 2); WC represents the total cloud mass in mixed-phase clouds,
 497 while LWC alone represents the total cloud mass in warm clouds.

Deleted: W...CC...that is lower than the time- and domain-averaged water contentcontent...(W...CC... which is the sum of IW...CC...and LW...CC... in mixed-phase clouds in the 200_2 run (Figure 4 and Table 2). Associated with this, the time- and domain-averaged LWP in the 200_2_noice run is lower than the time- and domain-averaged water path (WP), which is the sum of IWP and LWP, in the 200_2 run (Table 2). ...his is despite the fact that LWC and ...WP...C in the 200_2_noice run isare...higher than LWC and LWP...C, respectively, ...n the 200_2 run (Figure 4 and Table 2);...Here, WC (WP...C)...represents the total cloud mass in mixed-phase clouds, while LWC (...WP...C)...alone represents the total cloud mass in warm clouds. These results are also in contrast to the situation in the midlatitude case. The total cloud mass in warm clouds, which are generated by removing ice processes in the midlatitude case, is greater than that in the midlatitude case. ... [3]

498 It should be noted that the average rate of sedimentation of droplets over the cloud
 499 base and simulation period reduces from the 200_2_noice run to the 200_2 run (Table 2).
 500 This is mainly due to the decrease in LWC from the 200_2_noice run to the 200_2 run.
 501 The average rate of sedimentation of ice crystals over the cloud base and simulation period
 502 increases from the 200_2_noice run to the 200_2 run, since sedimentation of ice crystals is
 503 absent in the 200_2_noice run (Table 2). The average entrainment rate over the cloud top

Deleted: LWC or ...WP...C from the 200_2_noice run to the 200_2 run. The average rate of sedimentation of ice crystals over the cloud base and simulation period increases from the 200_2_noice run to the 200_2 run, since there is no ... [4]

618 and simulation period increases from the 200_2_noice run to the 200_2 run (Table 2).
 619 Hence, the droplet sedimentation tends to increase the total cloud mass in the 200_2 run,
 620 and the ice-crystal sedimentation and entrainment tend to reduce the total cloud mass in
 621 the 200_2 run, as compared to that in the 200_2_noice run. This means that the droplet
 622 sedimentation contributes to increase in the total cloud mass from the 200_2_noice run to
 623 the 200_2 run, while entrainment and the ice-crystal sedimentation counter the increase.
 624 Thus, entrainment and the ice-crystal sedimentation should be opted out when it comes to
 625 mechanisms leading to the increase in the total cloud mass. Here, the vertical integration
 626 of each of condensation and deposition rates is obtained over each cloudy column in the
 627 domain for each of the runs. For the sake of the brevity, this vertical integration of
 628 condensation (deposition) rate is referred to as the integrated condensation (deposition)
 629 rate. Then, each of the integrated condensation and deposition rates is averaged over cloudy
 630 columns and the simulation period. It is found that the change in the average rate of the
 631 droplet sedimentation over the cloud base and simulation period from the 200_2_noice run
 632 to the 200_2 run is ~five to six orders of magnitude smaller than that **in the average**
 633 **integrated condensation rate, the average integrated deposition rate, and the sum of the**
 634 **average integrated condensation and deposition rate** (Table 2). Thus, condensation and
 635 deposition, but not the droplet sedimentation, are main factors controlling differences in
 636 cloud mass, which is represented by LWC and IWC , and in the total cloud mass between
 637 the 200_2 and 200_2_noice runs as are between the midlatitude case and its warm-cloud
 638 counterpart.

640 **3.1.1 Hypothesis**

641
 642 We hypothesized that ICNC/CDNC can be an important factor that determines above-
 643 described differences between the polar and midlatitude cases. Remember that ice crystals
 644 **are more** as sources of deposition per a droplet when ICNC/CDNC is higher. Thus, when
 645 ICNC/CDNC is higher and $q_v > q_{sw}$, **it is more likely** that more portion of water vapor is
 646 deposited onto ice crystals by stealing water vapor, which is supposed to be condensed
 647 onto droplets, from droplets in an air parcel. Here, q_v and q_{sw} represent water-vapor
 648 pressure and water-vapor saturation pressure for liquid water or droplets, respectively.

Deleted: in

Deleted: rate and the average integrated

Deleted: in cloudy columns

Deleted: WP

Deleted: ,

Deleted:

Deleted: WP

Deleted: , and associated LWC and IWC

Deleted: 3.1.1

Formatted: Outline numbered + Level: 3 + Numbering
 Style: 1, 2, 3, ... + Start at: 1 + Alignment: Left + Aligned at:
 0.75" + Indent at: 1.25"

Deleted: there are more

Deleted: there is a higher possibility

660 When ICNC/CDNC is higher and $q_{si} < q_v < q_{sw}$, more ice crystals can absorb water vapor,
 661 including that which is produced by droplet evaporation, per a droplet; here, q_{si} represents
 662 water-vapor saturation pressure for ice water or ice crystals. Thus, with higher
 663 ICNC/CDNC, it is more likely that that more portion of water vapor is deposited onto ice
 664 crystals in an air parcel as shown in Lee et al. (2022).

Deleted: there are

Deleted: that

Deleted: there is a higher possibility

665 ICNCavg/CDNCavg is 0.22 in the control run (i.e., the 200_2 run) for the polar case
 666 and 0.019 in the control run for the midlatitude case which is described in Lee et al. (2022).

Formatted: Body Text 3, Left, Automatically adjust right indent when grid is defined, Adjust space between Latin and Asian text, Adjust space between Asian text and numbers

667 Henceforth, the control run for the midlatitude case is referred to as the control-midlatitude
 668 run. ICNCavg/CDNCavg is ~one order of magnitude higher for the polar case than for the
 669 midlatitude case. This is despite the fact that the ratio of the initial number concentration
 670 of aerosols acting as INP to that of acting as CCN is identical between the 200_2 and
 671 control-midlatitude runs. This is mainly due to the fact that ice nucleation strongly depends
 672 on air temperature (Prappacher and Klett, 1978). When supercooling is stronger, in general,

673 more ice crystals are nucleated for a given group of aerosols acting as INP. The average
 674 air temperature immediately below the cloud base over the simulation period is -16 °C in
 675 the 200_2 run and -5 °C in the control-midlatitude run. The average air temperature
 676 immediately above the cloud top is -33 °C in the 200_2 run and -15 °C in the control-

Deleted: there is

Deleted: nucleation of

677 midlatitude run. Hence, supercooling is greater and this contributes to the higher
 678 ICNCavg/CDNCavg in the polar case than in the midlatitude case. The higher
 679 ICNCavg/CDNCavg is likely to induce more portion of water vapor to be deposited onto
 680 ice crystals in the polar case than in the midlatitude case. It is hypothesized that this in turn

Deleted: there is more

Deleted: which

681 enables IWC/LWC in the 200_2 run to be one order of magnitude greater than that in the
 682 control-midlatitude run or in the midlatitude case. Much higher IWC than LWC, which
 683 results in a much higher IWC/LWC in the polar case than in the midlatitude case, in the
 684 200_2 run overcomes lower LWC in the 200_2 run than that in the 200_2 noise run, which
 685 leads to the greater total cloud mass in the 200_2 run than in the 200_2 noise run (Figure
 686 4 and Table 2). However, IWC whose magnitude is similar to the magnitude of LWC,
 687 which results in a much lower IWC/LWC in the midlatitude case than in the polar case, in
 688 the midlatitude case is not able to overcome lower LWC in the midlatitude case than that
 689 in the midlatitude warm clouds, which leads to the greater total cloud mass in the
 690 midlatitude warm clouds than in the midlatitude case; here, the midlatitude warm clouds

Deleted: IWC/LWC or

Deleted: WP

Deleted: WP

701 are generated by removing ice processes in the midlatitude case. This means that associated
 702 with higher ICNC/CDNC and IWC/LWC , ice processes enhance the total cloud mass for
 703 the polar case as compared to that for the polar warm-cloud counterpart. However, in the
 704 midlatitude case, associated with lower ICNC/CDNC and IWC/LWC , ice processes reduce
 705 the total cloud mass as compared to that for the midlatitude warm-cloud counterpart.

706

707 3.1.2 Role of ICNC/CDNC

708

709 To test the hypothesis above about the role of ICNC/CDNC in above-described differences
 710 between the polar and midlatitude cases, the 200_2 run is repeated by reducing
 711 ICNCavg/CDNCavg by a factor of 10. This is done by reducing the concentration of
 712 aerosols acting as INP but not CCN in a way that ICNCavg/CDNCavg is lower by a factor
 713 of 10 in the repeated run than in the 200_2 run. In this way, this repeated run has
 714 ICNCavg/CDNCavg at the same order of magnitude as that in the control-midlatitude run.
 715 This repeated run is referred to as the 200_2_fac10 run. As shown in Figure 6 and Table 2,
 716 the 200_2_fac10 run shows much lower deposition rate and IWC than the 200_2 run does.
 717 However, as we move from the 200_2 run to the 200_2_fac10 run, the time- and domain-
 718 averaged condensation rate and LWC increases (Figure 6 and Table 2). This is because
 719 reduction in deposition increases the amount of water vapor, which is not consumed by
 720 deposition but available for condensation. Associated with this, in the 200_2_fac10 run,
 721 the time- and domain-averaged deposition rate and IWC become similar to the average
 722 condensation rate and LWC , respectively (Figure 6 and Table 2). Hence, IWC/LWC
 723 reduces from 26.28 in the 200_2 run to 1.05 in the 200_2_fac10 run as ICNCavg/CDNCavg
 724 reduces from the 200_2 run to the 200_2_fac10 run. Here, IWC/LWC in the 200_2_fac10
 725 run is similar to that in the midlatitude-control run, which demonstrate that the difference
 726 in ICNC/CDNC is able to explain the difference in IWC/LWC between the polar and
 727 midlatitude cases. It is notable that the reduction in deposition is dominant over the increase
 728 in condensation with the decrease in ICNCavg/CDNCavg. Hence, the sum of condensation
 729 and deposition rates and WC reduce from the 200_2 run to the 200_2_fac10 run. That the
 730 sum of condensation and deposition rates and WC reduce in a way that the sum and WC in
 731 the mixed-phase clouds in the 200_2_fac10 run are lower than condensation rate and LWC .

Deleted: Higher IWC/LWC (IWP/LWP) results in WC (WP) in the 200_2 run which is greater than LWC (LWP) in the warm clouds in the 200_2_noise run, while lower IWC/LWC (IWP/LWP) results in WC (WP) in the midlatitude mixed-phase clouds which is lower than LWC (LWP) in their warm-cloud counterpart.

Deleted: , IWC/LWC

Deleted: WP

Deleted: WP

Deleted: , IWC/LWC

Deleted: WP

Deleted: WP

Deleted: , IWC and

Deleted: WP

Deleted: , LWC

Deleted: WP

Deleted: , IWC and

Deleted: WP

Deleted: , LWC

Deleted: WP

Deleted: IWC/LWC and

Deleted: WP

Deleted: WP

Deleted: 26.28 and

Deleted: 5

Deleted: 96

Deleted: 1.05 and

Deleted: 2

Deleted: , respectively,

Deleted: IWC/LWC and

Deleted: WP

Deleted: WP

Deleted: are

Deleted: ose

Deleted: IWC/LWC and

Deleted: WP

Deleted: WP

Deleted: , WC and WP

Deleted: It is also notable that t

Deleted: , WC

Deleted: WP

Deleted: , WC and WP

Deleted: , LWC

Deleted: WP

775 **respectively**, in the warm clouds in the 200_2_noice run **is also notable** (Figure 6 and Table
 776 2). This is similar to the situation in the midlatitude case and thus demonstrates that the
 777 different relation between the mixed-phase and warm clouds can **be associated with** the
 778 difference in ICNC/CDNC between the polar and midlatitude cases.

779 The rate of the sedimentation of ice crystals at the cloud base reduces as
 780 ICNCavg/CDNCavg reduces between the 200_2 and 200_2_fac10 runs, mainly due to
 781 reduction in the ice-crystal mass (Table 2). The rate of droplet sedimentation at the cloud
 782 base increases as ICNCavg/CDNCavg reduces mainly due to increases in droplet mass and
 783 size in association with the increases in **LWC** (Table 2). The entrainment rate at the cloud
 784 top reduces as ICNCavg/CDNCavg reduces (Table 2). Hence, the changing sedimentation
 785 tends to reduce **LWC** and increase **IWC**, while the changing entrainment tends to increase
 786 the total cloud mass **or WVC** with the reducing ICNCavg/CDNCavg. Hence, changes in the
 787 sedimentation counter the increase in **LWC**, and the decrease in **IWC** with the reducing
 788 ICNCavg/CDNCavg. Changes in the entrainment counters the decrease in **WVC** with the
 789 reducing ICNCavg/CDNCavg between the 200_2 and 200_2_fac10 runs. Here, we see that
 790 changes in the sedimentation and entrainment are not factors that lead to the increase in
 791 **LWC**, and the decrease in **IWC**, and eventually the decrease in **WVC** with the reducing
 792 ICNCavg/CDNCavg. The analysis of the sedimentation and entrainment exclude them
 793 from factors inducing above-described differences between the 200_2 and 200_2_fac10
 794 runs. Instead, this analysis grants more confidence in the fact that deposition and
 795 condensation, which are strongly dependent on ICNC/CDNC, are main factors inducing
 796 those differences.

798 **3.2 Aerosol-cloud interactions**

800 Comparisons between the 200_2 and 2000_20 runs show that with the increasing
 801 concentration of both of aerosols acting as CCN and those as INP, **IWC increases** but **LWC**
 802 **decreases** in the polar case (Figures 7 and Table 2). These decreases in **LWC** are negligible
 803 as compared to these increases in **IWC**. Hence, the increases in **IWC** outweigh the
 804 decreases in **LWC**, leading to aerosol-induced increases in **WVC** (Figures 7 and Table 2).
 805 To identify roles of specific types of aerosols in these aerosol-induced changes,

Deleted: , respectively

Deleted: e explained by

Deleted: LWC and

Deleted: WP

Deleted: LWC or

Deleted: WP

Deleted: IWC or

Deleted: WP

Deleted: ,

Deleted: WC or WP

Deleted: LWC or

Deleted: WP

Deleted: IWC or

Deleted: WP

Deleted: WC or WP

Deleted: LWC or

Deleted: WP

Deleted: IWC or

Deleted: WP

Deleted: WP

Deleted: ¶

Deleted: 3.2

Formatted: Font: Bold

Formatted: List Paragraph, Outline numbered + Level: 2 +
 Numbering Style: 1, 2, 3, ... + Start at: 1 + Alignment: Left +
 Aligned at: 0.5" + Indent at: 0.75"

Deleted: there are increases in IWC and

Deleted: WP

Deleted: decreases in LWC and

Deleted: WP

Deleted: LWC and

Deleted: WP

Deleted: IWC and

Deleted: WP

Deleted: IWC and

Deleted: WP

Deleted: LWC and

Deleted: WP

Deleted: WC and WP

Deleted: , respectively

842 comparisons not only between the 200_2 and 200_20 runs but also between the 200_2 and
 843 2000_2 runs are performed. Comparisons between the 200_2 and 200_20 runs show that
 844 the increasing concentration of aerosols acting as INP induces increases in IWC but
 845 decreases in LWC (Figure 7 and Table 2). The magnitudes of these increases and decreases
 846 are similar to those between the 200_2 and 2000_20 runs (Figure 7 and Table 2). However,
 847 comparisons between the 200_2 and 2000_2 runs show that the increasing concentration
 848 of aerosols acting as CCN induces negligible changes in either IWC or LWC . Thus, CCN-
 849 induced changes in the total cloud mass **are negligible**, although the increasing
 850 concentration of aerosols acting as CCN induces a slight decrease in IWC , and a slight
 851 increase in LWC (Figure 7 and Table 2). This demonstrates that INP plays a much more
 852 important role than CCN when it comes to the response of the total cloud mass to increasing
 853 aerosol concentrations. However, in the midlatitude case, the increasing concentration of
 854 aerosols acting as CCN generates changes in the mass as significantly as the increasing
 855 concentration of aerosols acting as INP does.

856 To identify roles played by ice processes in aerosol-cloud interactions, a pair of the
 857 200_2_noice and 2000_2_noice runs are analyzed and compared to the previous four
 858 standard simulations (i.e., the 200_2, 200_20, 2000_2 and 2000_20 runs). The CCN-
 859 induced increases in LWC in those noice runs are much greater than the CCN-induced
 860 changes in WC in the 200_2 and 2000_2 runs (Figure 7 and Table 2). However, these CCN-
 861 induced increases in IWC in the noice runs are smaller than the INP-induced increases in
 862 WC in the 200_2 and 200_20 runs (Figure 7 and Table 2). This is different from the
 863 midlatitude case where changes in the total cloud mass, whether they are induced by the
 864 increasing concentration of aerosols acting as CCN or INP, in the mixed-phase clouds are
 865 much lower than those CCN-induced changes in the warm clouds.

866

867 3.2.1 Deposition, condensation, sedimentation and entrainment

868

869 The CCN-induced increases (decreases) in condensation (deposition) rate **are negligible**,
 870 leading to the CCN-induced negligible increases (decreases) in IWC (IWC) between the
 871 200_2 and 2000_2 runs (Figure 7 and Table 2). However, between the 200_2 and 200_20
 872 runs, rather the significant INP-induced increases **are** in deposition rate, leading to the

Deleted: IWC and

Deleted: WP

Deleted: LWC and

Deleted: WP

Deleted: a pair of IWC and

Deleted: WP

Deleted: a pair of LWC and

Deleted: WP

Deleted: there are negligible

Deleted: IWC and

Deleted: WP

Deleted: LWC and

Deleted: WP

Deleted: liquid, ice and

Deleted: LWC and

Deleted: WP

Deleted: WC and WP

Deleted: , respectively,

Deleted: LWC and

Deleted: WP

Deleted: WC and WP

Deleted: , respectively,

Deleted: There are

Deleted: t

Deleted: negligible

Deleted: LWC and

Deleted: WP

Deleted: IWC and

Deleted: WP

Deleted: there are

903 significant INP-induced increases in IWC (Figure 7 and Table 2). Between the 200_2 and
 904 200_20 runs, INP-induced decreases in condensation rate are negligible, leading to the
 905 negligible INP-induced decreases in LWC , as compared to the INP-induced increases in
 906 deposition rate and IWC (Figure 7 and Table 2). With the increasing concentration of
 907 aerosols acting as INP from the 200_2 run to the 200_20 run, the sedimentation of ice
 908 crystals at the cloud base decreases (Table 2). This is mainly due to decreases in the size
 909 of ice crystals in association with increases INP and resultant increases in ICNC. From the
 910 200_2 run to the 200_20 run, the sedimentation of droplets at the cloud base decreases as
 911 shown in Table 2, mainly due to decreases in LWC . From the 200_2 run to the 200_20 run,
 912 the entrainment at the cloud top increases (Table 2). Hence, the INP-induced changes in
 913 the sedimentation contribute to the INP-induced increases in IWC but counter the INP-
 914 induced reduction in LWC . The entrainment counters the INP-induced increases in IWC .
 915 Hence, we see that changes in entrainment and the droplet sedimentation are not factors
 916 that lead to the INP-induced increases in IWC and decreases in LWC , respectively. The
 917 INP-induced increases in deposition and decreases in the sedimentation of ice crystals both
 918 contribute to the INP-induced increases in IWC . However, the INP-induced changes in the
 919 average integrated deposition rate over cloudy columns and the simulation period is ~ four
 920 orders of magnitude greater than those in the average rate of ice-crystal sedimentation over
 921 the cloud base and simulation period (Table 2). Hence, the role of the ice-crystal
 922 sedimentation in the INP-induced changes in IWC is negligible as compared to that of
 923 deposition.

924 In the warm clouds in the 200_2_noice and 2000_2_noice runs, the CCN-induced
 925 increases in condensation rate occur, leading to those in LWC (Figure 7 and Table 2).
 926 However, the CCN-induced increases in condensation rate in the warm clouds associated
 927 with the polar case are lower than the INP-induced increases in deposition rate in the polar
 928 case (Table 2). This contributes to aerosol-induced smaller changes in the total cloud mass
 929 in the polar warm clouds than in the polar mixed-phase clouds. The sedimentation of
 930 droplets at the cloud base reduces and the entrainment at the cloud top increases from the
 931 200_2_noice run to 2000_2_noice run (Table 2). The increasing concentration of aerosols
 932 acting as CCN induces increases in CDNC and decreases in the droplet size, leading to the
 933 reduction in the droplet sedimentation from the 200_2_noice run to 2000_2_noice run. The

Deleted: IWC and

Deleted: WP

Deleted: there are negligible

Deleted: LWC and

Deleted: WP

Deleted: , IWC

Deleted: WP

Deleted: there are decreases in

Deleted: there are decreases in

Deleted: LWC or

Deleted: WP

Deleted: there are increases in

Deleted: IWC or

Deleted: WP

Deleted: LWC or

Deleted: WP

Deleted: WC or WP

Deleted: WC (WP

Deleted:)

Deleted: LWC (

Deleted: WP

Deleted:)

Deleted: IWC and

Deleted: WP

Deleted: at

Deleted: IWC and

Deleted: WP

Deleted: there are

Deleted: LWC and

Deleted: WP

964 CCN-induced changes in the sedimentation contribute to the CCN-induced increases in
 965 LWC . The entrainment counters the CCN-induced increases in LWC . Hence, the
 966 entrainment is not a factor which induces the CCN-induced increases in LWC between the
 967 200_2_noice and 2000_2_noice runs. As seen in Table 2, the CCN-induced changes in the
 968 sedimentation rate are \sim three orders of magnitude smaller than those in the integrated
 969 condensation rate. Hence, the role of sedimentation in changes in LWC or WC between
 970 the 200_2_noice and 2000_2_noice runs is negligible as compared to that of condensation.

971

972 **3.2.2 Understanding differences between the polar and midlatitude cases**

973

974 Roughly speaking, the CCN-(INP-)induced changes in LWC (IWC) via CCN-
 975 (INP-)induced changes in autoconversion of droplets (ice crystals) are proportional to
 976 LWC (IWC) that changing CCN (INPs) affect (e.g., Liu and Daum, 2004; Kogan, 2013;
 977 Lee and Baik, 2017; Dudhia, 1989; Lim and Hong, 2010; Mansell et al. 2010). This is for
 978 given environmental conditions (e.g., temperature and humidity) and given CCN-
 979 (INP-)induced changes in microphysical factors such as sizes and number concentrations
 980 of droplets (ice crystals). Hence, in the polar case, with a given much lower LWC than
 981 IWC , the changing concentration of aerosols acting as CCN is likely to induce smaller
 982 changes in the given LWC via CCN impacts on the droplet autoconversion. This is as
 983 compared to changes in the given IWC which are induced by the changing concentration
 984 of aerosols acting as INP and thus changing ice-crystal autoconversion.

985 The smaller (larger) changes in the given LWC (IWC) are related to changes in CDNC
 986 (ICNC). These changes in CDNC (ICNC) are initiated by those in droplet (ice crystal)
 987 autoconversion. Changes in integrated droplet (ice-crystal) surface area, which are induced
 988 by those in CDNC (ICNC), initiate those in the given LWC (IWC). Remember that
 989 condensation (deposition) occurs on droplet (ice-crystal) surface and thus droplets (ice
 990 crystals) act as a source of condensation (deposition). Hence, those changes in CDNC
 991 (ICNC) and associated integrated droplet (ice-crystal) surface area can lead to changes in
 992 condensation (deposition) and thus feedbacks between condensation (deposition) and
 993 updrafts. The smaller CCN-induced changes in LWC involve changes in CDNC and
 994 associated smaller changes in condensation and feedbacks between condensation and

~~Deleted: LWC and~~~~Deleted: WP~~~~Deleted: LWC or~~~~Deleted: WP~~~~Deleted: LWC or~~~~Deleted: WP~~~~Deleted:~~~~Deleted: LWP or WP~~~~Deleted: 3.2.2~~~~Formatted: Outline numbered + Level: 3 + Numbering Style: 1, 2, 3, ... + Start at: 1 + Alignment: Left + Aligned at: 0.5" + Indent at: 1"~~~~Deleted: LWC (IWC) or~~~~Deleted: WP~~~~Deleted: WP~~~~Deleted: LWC (IWC) or~~~~Deleted: WP~~~~Deleted: WP~~~~Deleted: (~~~~Deleted:)~~~~Deleted: (~~~~Deleted:)~~~~Deleted: (~~~~Deleted:)~~~~Deleted: LWC (~~~~Deleted: WP~~~~Deleted:)~~~~Deleted: IWC (~~~~Deleted: WP~~~~Deleted:)~~~~Deleted: LWC (~~~~Deleted: WP~~~~Deleted:)~~~~Deleted: IWC or~~~~Deleted: WP~~~~Deleted: LWC or LWP (IWC or~~~~Deleted:~~~~Deleted: WP~~~~Deleted:)~~~~Deleted: , which are initiated by those in droplet (ice crystal) autoconversion, and associated integrated droplet (ice-crystal) surface area.~~~~Deleted: LWC or~~~~Deleted: WP~~~~Deleted: associated~~

1037 updrafts in the polar case. This is as compared to changes in deposition and feedbacks
 1038 between deposition and updrafts which are associated with the INP-induced changes in
 1039 ICNC and the related larger INP-induced changes in IWC in the polar case. The smaller
 1040 CCN-induced changes in LWC involve smaller changes in water vapor that is consumed
 1041 by droplets in the polar case. The larger INP-induced changes in IWC involve larger
 1042 changes in water vapor that is consumed by ice crystals in the polar case. This leaves the
 1043 CCN-induced smaller changes in the amount of water vapor available for deposition, which
 1044 induce the smaller CCN-induced changes in IWC in the polar case. This is as compared to
 1045 the INP-induced changes in the amount of water vapor which is available for condensation
 1046 and associated changes in LWC in the polar case.

Deleted: IWC and $\dots WP \dots C$ in the polar case. The smaller CCN-induced changes in LWC (or $\dots WP \dots C$)...involve smaller changes in water vapor that is consumed by droplets in the polar case. The larger INP-induced changes in IWC (or $\dots WP \dots C$)...involve larger changes in water vapor that is consumed by ice crystals in the polar case. This leaves the CCN-induced smaller changes in the amount of water vapor available for deposition, which induce the smaller CCN-induced changes in IWC and $\dots WP \dots C$ in the polar case. This is as compared to the INP-induced changes in the amount of water vapor which is available for condensation and associated changes in LWC or $\dots WP \dots$... [5]

1047 The lower LWC in the polar warm clouds than IWC in the polar case contributes to the
 1048 INP-induced greater changes in IWC than the CCN-induced changes in LWC in the polar
 1049 warm clouds. The lower LWC in the polar case than that in the polar warm clouds
 1050 contributes to the CCN-induced greater changes in LWC in the polar warm clouds than
 1051 those in LWC and subsequent changes in IWC in the polar case.

Deleted: LWC ($\dots WP \dots C$)...in the polar warm clouds than IWC ($\dots WP \dots C$)...in the polar case contributes to the INP-induced greater changes in IWC ($\dots WP \dots C$)...than the CCN-induced changes in LWC ($\dots WP \dots C$)...in the polar warm clouds. The lower LWC ($\dots WP \dots C$)...in the polar case than that in the polar warm clouds contributes to the CCN-induced greater changes in LWC ($\dots WP \dots C$)...in the polar warm clouds than those in LWC ($\dots WP \dots C$)...and subsequent changes in IWC ($\dots WP \dots C$) ... [6]

1052 In contrast to the situation in the polar case, in the midlatitude case, remember that a
 1053 given LWC is at the same order of magnitude of IWC . Hence, the CCN-induced changes
 1054 in LWC and subsequent changes in IWC are similar to the INP-induced changes in IWC
 1055 and subsequent changes in LWC . The greater LWC in the midlatitude warm cloud than
 1056 both of LWC and IWC in the midlatitude case contributes to the greater CCN-induced
 1057 changes in LWC in the midlatitude warm cloud. This is as compared to either the CCN-
 1058 induced changes in LWC and subsequent changes in IWC or the INP-induced changes in
 1059 IWC and subsequent changes in LWC in the midlatitude case.

Deleted: ...n contrast to the situation in the polar case, in the midlatitude case, remember that a given LWC ($\dots WP \dots C$)...is at the same order of magnitude of IWC ($\dots WP \dots C$)... Hence, the CCN-induced changes in LWC ($\dots WP \dots C$)...and subsequent changes in IWC ($\dots WP \dots C$)...are similar to the INP-induced changes in IWC ($\dots WP \dots C$)...and subsequent changes in LWC ($\dots WP \dots C$)... The greater LWC ($\dots WP \dots C$)...in the midlatitude warm cloud than both of LWC ($\dots WP \dots C$)...and IWC ($\dots WP \dots C$)...in the midlatitude case contributes to the greater CCN-induced changes in LWC ($\dots WP \dots C$)...in the midlatitude warm cloud. This is as compared to either the CCN-induced changes in LWC ($\dots WP \dots C$)...and subsequent changes in IWC ($\dots WP \dots C$)...or the INP-induced changes in IWC ($\dots WP \dots C$)...and subsequent changes in LWC ($\dots WP \dots C$)... ... [7]

1060 To confirm above-described mechanisms in this section, which explain different
 1061 aerosol-cloud interactions between the polar and midlatitude cases, the 200_2_fac10 run is
 1062 repeated by increasing INP by a factor of 10 in the PBL at the first time step. This repeated
 1063 run is referred to as “the 200_2_fac10_INP10 run. Then, the 200_2_fac10 run is repeated
 1064 again by increasing CCN by a factor of 10 in the PBL at the first time step. This repeated
 1065 run is referred to as the 200_2_fac10_CCN10 run. These repeated runs are to see the
 1066 response of IWC and LWC to the increasing concentration of aerosols acting as INP and
 1067 CCN. This is when IWC and LWC are at the same order of magnitude and lower in mixed-

Deleted: ...o confirm above-described mechanisms in this section, which explain different aerosol-cloud interactions between the polar and midlatitude cases, the 200_2_fac10 run is repeated by increasing INP by a factor of 10 in the PBL at the first time step. This repeated run is referred to as “the 200_2_fac10_INP10 run. Then, the 200_2_fac10 run is repeated again by increasing CCN by a factor of 10 in the PBL at the first time step. This repeated run is referred to as the 200_2_fac10_CCN10 run. These repeated runs are to see the response of IWC , $\dots W \dots C$, LWC ...nd $LWP \dots C$ to the increasing concentration of aerosols acting as INP and CCN. This is when IWC ($\dots WP \dots C$)...and LWC ($\dots WP \dots C$) ... [8]

1202 phase clouds than ~~LWC~~ in the warm-cloud counterpart as in the 200_2_fac10 run and
 1203 midlatitude case. Comparisons between the 200_2_fac10, 200_2_fac10_INP10 and
 1204 200_2_fac10_CCN10 runs show that the INP-induced changes in ~~IWC~~ and ~~LWC~~ are
 1205 similar to the CCN-induced changes in ~~IWC~~ and ~~LWC~~, respectively, as in the midlatitude
 1206 case. These comparisons also show that the CCN-induced changes in ~~LWC~~ in the polar
 1207 warm cloud are greater. This is as compared to either the CCN-induced changes in ~~LWC~~,
 1208 and subsequent changes in ~~IWC~~ between the 200_2_fac10 and 200_2_fac10_CCN10 runs
 1209 or the INP-induced changes in ~~IWC~~ and subsequent changes in ~~LWC~~ between the
 1210 200_2_fac10 and 200_2_fac10_INP10 runs. These comparisons demonstrate that
 1211 differences in ICNC/CDNC play a critical role in differences in aerosol-cloud interactions
 1212 between the polar and midlatitude cases, considering that differences in ICNC/CDNC
 1213 between the 200_2 and 200_2_fac10 runs are at the same order of magnitude of those
 1214 between the cases.

1216 3.3 Radiation

1217
 1218 Studies (e.g., Ovchinnikov et al., 2011; Possner et al., 2017; Solomon et al., 2018) have
 1219 focused on radiative cooling and subsequent changes in stability and dynamics as a primary
 1220 driver for the development of mixed-phase stratocumulus clouds and aerosol-induced
 1221 changes in LWC and IWC in those clouds. Motivated by these studies, to isolate the role
 1222 of radiative processes in cloud development and aerosol impacts on LWC and IWC, all of
 1223 the simulations above are repeated by turning off radiative processes. In these repeated
 1224 runs, radiative fluxes over the whole domain and simulation period are zero. The basic
 1225 summary of results from these repeated runs is given in Table 3. As seen in comparisons
 1226 between Tables 2 and 3, the qualitative nature of results, which are mainly about
 1227 differences in IWC/LWC, the relative importance of the impacts of INP on IWC and LWC
 1228 as compared to those impacts of CCN, and how warm and mixed-phase clouds are related
 1229 between the polar and midlatitude cases, in this study does not vary with whether radiative
 1230 processes exist or not. This demonstrates that ICNC, CDNC, deposition and condensation
 1231 but not radiative processes drive results in this study.
 1232

Deleted: LWC (

Deleted: WP

Deleted:)

Deleted: IWC (

Deleted: WP

Deleted:)

Deleted: LWC (

Deleted: WP

Deleted:)

Deleted: at the same order of magnitude of

Deleted: IWC (

Deleted: WP

Deleted:)

Deleted: LWC (

Deleted: WP

Deleted:)

Deleted: LWC (

Deleted: WP

Deleted:)

Deleted: LWC (

Deleted: WP

Deleted:)

Deleted: IWC (

Deleted: WP

Deleted:)

Deleted: IWC (

Deleted: WP

Deleted:)

Deleted: LWC (

Deleted: WP

Deleted:)

Deleted: at

Formatted: Outline numbered + Level: 2 + Numbering
 Style: 1, 2, 3, ... + Start at: 2 + Alignment: Left + Aligned at:
 0.25" + Indent at: 0.58"

Formatted: Font: (Default) Times New Roman, (Asian)
 Malign Gothic, 12 pt, Font color: Auto

Formatted: Font: (Default) Times New Roman, (Asian)
 Malign Gothic, 12 pt, Font color: Auto

Formatted: Font: (Default) Times New Roman, (Asian)
 Malign Gothic, 12 pt, Font color: Auto

4. Discussion

4.1 Examination of the role of ICNC/CDNC in IWC/LWC in 200_2, 2000_20, 2000_2, 200_20, 200_2 fac10, 200_2 fac10 CCN10 and 200_2 fac10 INP10 runs

So far, comparisons between the set of the 200_2, 2000_20, 2000_2 and 200_20 runs for the polar case and the other set of the 200_2 fac10, 200_2 fac10 CCN10 and 200_2 fac10 INP10 runs, which represents the midlatitude case, have been mainly utilized to understand the role of ICNC/CDNC. However, even when it comes to all the runs in both the sets, differences in ICNCavg/CDNCavg and IWC/LWC are shown among them (Tables 1 and 2). For more robust examination of particularly the role of ICNC/CDNC in IWC/LWC, which is basically about the increase (decrease) in ICNC/CDNC inducing the increase (decrease) in IWC/LWC as identified from the comparison between the 200_2 and 200_2 fac10 runs in Section 3.1.2, all the runs in the sets are utilized by ordering them as shown in Table 4. This ordering is done in a way that as we move from the first run in the first row to the last run in the last row of Table 4, ICNCavg/CDNCavg increases. Overall, with increasing ICNCavg/CDNCavg, IWC/LWC increases, although the increase in IWC/LWC is highly non-linear in terms of the increase in ICNCavg/CDNCavg as seen in the percentage increases, and a decrease in IWC/LWC is seen with an increase in ICNCavg/CDNCavg from the 2000_20 run to the 200_2 run (Table 4); this high-degree non-linearity in the increase in IWC/LWC is associated with the fact that interactions between cloud microphysical, thermodynamic and dynamic processes are well known to be highly non-linear. Hence, overall, findings regarding the role of ICNC/CDNC in IWC/LWC from the comparison between the 200_2 and 200_2 fac10 runs are applicable to all the runs in the sets except for the role between the 2000_20 and 200_2 runs. Here, it is notable that the percentage difference in ICNCavg/CDNCavg is ~9% between the 2000_20 and 200_2 runs and the smallest among those differences in Table 4. The other differences are larger than 80%. Hence, the percentage difference in ICNCavg/CDNCavg for a pair of the 2000_20 and 200_2 runs is at least ~one order of magnitude smaller than that for the other pairs of the runs in Table 4. This means that findings from the comparison

Formatted: Font: Bold

Formatted: Outline numbered + Level: 1 + Numbering Style: 1, 2, 3, ... + Start at: 1 + Alignment: Left + Aligned at: 0.25" + Indent at: 0.5"

Deleted: ¶

Formatted: Font: Bold

Formatted: Font: Bold

Formatted: Font: Bold

Formatted: Font: Bold

Formatted: Indent: Left: 0.75"

1297 between the 200_2 and 200_2_fac10 runs are not suitable to explain the variation of
 1298 IWC/LWC among clouds when the variation of ICNC/CDNC is relatively insignificant.
 1299 According to Table 4, it seems that the variation of ICNC/CDNC should be greater than a
 1300 critical value above which those findings are useful to account for the IWC/LWC variation
 1301 among clouds.

1302

1303 4.2 Role of a given ICNC/CDNC in IWC/LWC for different concentrations of 1304 aerosols acting as INP and CCN

1305

1306 Simulations which are compared in Section 4.1 and shown in Table 4 have not only
 1307 different ICNCavg/CDNCavg but also the different number concentrations of aerosols
 1308 acting as CCN and INP at the first time step (Table 1). To better isolate particularly the
 1309 role of ICNC/CDNC in IWC/LWC, we need to show that results in Section 4.1 are valid
 1310 regardless of the variation of the number concentration of aerosols. For this need, we focus
 1311 on the 200_2 and 200_2_fac10 runs, since the primary understanding of the role of
 1312 ICNC/CDNC in IWC/LWC comes from the comparison between these runs as described
 1313 in Section 3.1.2. To fulfill the need, each of these runs are repeated by varying the number
 1314 concentration of aerosols acting as CCN and INP in a way that ICNCavg/CDNCavg does
 1315 not vary (Tables 1 and 5). The 4000_45 and 13_0.1 runs are the repeated 200_2 run, and
 1316 the 4000_1.8_fac10 and 12_0.0035_fac10 runs are the repeated 200_2_fac10 run (Tables
 1317 1 and 5). The set of the 200_2, 4000_45 and 13_0.1 runs is referred to as the polar set, and
 1318 that of the 200_2_fac10, 4000_1.8_fac10 and 12_0.0035_fac10 runs is referred to as the
 1319 midlatitude set in this section. Among the three runs in each of the sets, less than 4%
 1320 variation of IWC/LWC is shown (Table 5). This less-than-4% variation is so small that the
 1321 start contrast in IWC/LWC between the 200_2 and 200_2_fac10 runs as discussed in
 1322 Section 3.1.2 is also shown between the polar and midlatitude sets (Table 5). Hence, the
 1323 role of the difference in a given ICNC/CDNC in the difference in IWC/LWC between the
 1324 200_2 and 200_2_fac10 runs as described in Section 3.1.2 is considered robust to the
 1325 varying concentration of aerosols.

1326

1327 5. Summary and conclusions

Formatted: Outline numbered + Level: 2 + Numbering
 Style: 1, 2, 3, ... + Start at: 2 + Alignment: Left + Aligned at:
 0.5" + Indent at: 0.75"

Deleted: ¶

1329
 1330 In this study, a case of mixed-phase clouds in a polar area, which is referred to as “the polar
 1331 case” is compared to that in a midlatitude area, which is referred to as “the midlatitude
 1332 case”. This is to gain an understanding of how different ICNC/CDNC plays a role in
 1333 making differences in cloud properties, aerosol-cloud interactions, and impacts of ice
 1334 processes on them between two representative areas (i.e., polar and midlatitude areas)
 1335 where mixed-phase stratiform clouds form and develop. Among those cloud properties,
 1336 this study focuses on IWC/LWC that plays an important role in cloud radiative properties.
 1337 To gain the understanding efficiently, the polar case is chosen in a way to make stark
 1338 contrast with the midlatitude case in terms of ICNC/CDNC and IWC/LWC. Although such
 1339 polar cases may be uncommon, the stark contrast provides an opportunity to elucidate
 1340 mechanisms that control the above-mentioned role of different ICNC/CDNC.

Deleted: their interactions with

Deleted: s

Deleted: is IWC/LWC or

Deleted: WP

Deleted: WP

1341 Due to lower air temperature, more ice crystals are nucleated, leading to higher
 1342 ICNC/CDNC in the polar case than in the midlatitude case. This higher ICNC/CDNC
 1343 enables the more efficient deposition of water vapor onto ice crystals in the polar case. This
 1344 leads to much higher IWC/LWC in the polar case. The more efficient deposition of water
 1345 vapor onto ice crystals enables the polar mixed-phase clouds to have the greater total cloud
 1346 mass than the polar warm clouds. However, the less efficient deposition of water vapor
 1347 onto ice crystals causes the midlatitude mixed-phase clouds to have less total cloud mass
 1348 than the midlatitude warm clouds. With the increasing ICNC/CDNC from the midlatitude
 1349 case to the polar case, impacts of CCN (IFN) on the total cloud mass become less (more)
 1350 important.

Deleted: IWC/LWC or

Deleted: WP

Deleted: WP

1351 This study picked ICNC/CDNC, which is affected by air temperature and its impacts
 1352 on ice-crystal nucleation, as an important factor which differentiates IWC/LWC and
 1353 interactions among clouds, aerosols and ice processes in the polar area from those in the
 1354 midlatitude area. Differences in ICNC/CDNC initiate differences in the microphysical
 1355 properties (e.g., the integrated surface area), and then, subsequently induce those in
 1356 thermodynamic latent-heat processes (e.g., condensation and deposition), dynamics of
 1357 clouds, IWC/LWC and interactions among clouds, aerosols and ice processes. However,
 1358 this does not mean that no other potential factors, which can explain the variation of
 1359 IWC/LWC and interactions among clouds, aerosols and ice processes between those areas.

Deleted: among cloud properties,

Deleted: and

Deleted: s

Deleted: there are

Deleted: cloud properties

Deleted:

Deleted: among those properties,

1375 ~~exist.~~ For example, differences in environmental factors (e.g., stability and wind shear)
 1376 between the areas can have an impact on the variation. Particularly, differences in stability
 1377 and wind shear can initiate those in the dynamic development of turbulence. Then, this
 1378 subsequently induces differences in the microphysical and thermodynamic development of
 1379 clouds, IWC/LWC and interactions among clouds, aerosols and ice processes. Hence,
 1380 factors such as stability and wind shear can have different orders of procedures, which
 1381 involve dynamics, thermodynamics and microphysics, than ICNC/CDNC in terms of
 1382 differentiation between the polar and midlatitude mixed-phase clouds. Thus, different
 1383 mechanisms controlling the differentiation can be expected regarding factors such as
 1384 stability and wind shear as compared to ICNC/CDNC. The examination of these different
 1385 mechanisms among stability, wind shear and ICNC/CDNC deserves future study for more
 1386 comprehensive understanding of the differentiation.

1387 Another point to make is that the cases in this study have weak precipitation and the
 1388 associated weak sedimentation of ice crystals and droplets. In mixed-phase clouds with
 1389 strong precipitation and the sedimentation, they can play roles as important as in-cloud
 1390 latent-heat processes in IWC/LWC, and interactions among clouds, aerosols and ice
 1391 processes. In those clouds with strong precipitation, the sedimentation can take part in the
 1392 interplay between ICNC/CDNC and latent-heat processes by affecting cloud mass and
 1393 associated ICNC and CDNC significantly, and play a role in the differentiation of
 1394 IWC/LWC, and interactions among clouds, aerosols and ice processes when it comes to
 1395 different cases of mixed-phase clouds. For more generalization of results here, this
 1396 potential role of sedimentation needs to be investigated by performing more case studies
 1397 involving cases with strong precipitation in the future.

1398 It should be emphasized that although this study mentions air temperature as a factor
 1399 that affects ICNC/CDNC, ICNC/CDNC can be affected by other factors such as sources of
 1400 aerosols acting as INP and those acting as CCN, and/or the advection of those aerosols.
 1401 Hence, even for cloud systems that develop with a similar air-temperature condition, for
 1402 example, when those systems are affected by different sources of aerosols and/or their
 1403 different advection, they are likely to have different ICNC/CDNC, IWC/LWC, relative
 1404 importance of impacts of INP on IWC and LWC as compared to those impacts of CCN,
 1405 and relation between warm and mixed-phase clouds.

Deleted:

Deleted: cloud development

Deleted: ,

Deleted: s

Deleted: among clouds,

Deleted: , and their variation among different cases of mixed-phase clouds

Deleted: Hence, i

Deleted: cloud properties

Deleted: among those properties,

Deleted:

Deleted: WP

Deleted: WP

Deleted: and

Deleted: and CCN

Deleted: WP

Deleted: WP

Deleted: .

1424 Previous studies on mixed-phase stratocumulus clouds (e.g., Ovchinnikov et al., 2011;
 1425 Possner et al., 2017; Solomon et al., 2018) have primarily focused on investigating the
 1426 impacts of cloud-top radiative cooling, entrainment, and sedimentation of ice particles on
 1427 these clouds, as well as their interactions with aerosols. However, there are a scarcity of
 1428 studies that specifically examine the role of microphysical interactions, involving
 1429 processes such as condensation and deposition, as well as factors like cloud-particle
 1430 concentrations, between ice and liquid particles in mixed-phase stratocumulus clouds, and
 1431 their interactions with aerosols as performed in this study. Therefore, our study contributes
 1432 to a more comprehensive understanding of mixed-phase clouds and their intricate interplay
 1433 with aerosols.

1434 This study suggests that a microphysical factor, which is ICNC/CDNC, can be a
 1435 simplified and useful tool to understand differences among different systems of
 1436 stratocumulus clouds in various regions in terms of IWC/LWC and the relative importance
 1437 of INP and CCN in aerosol-cloud interactions, and thus to contribute to the development
 1438 of general parameterizations of those clouds in various regions for climate models. This
 1439 factor can also be a useful tool for a simplified understanding of different roles of ice
 1440 processes when mixed-phase clouds are compared to their warm-cloud counterparts in
 1441 terms of the cloud development and its interactions with aerosols among those different
 1442 systems. It should be noted that warm clouds have been studied much more than mixed-
 1443 phase clouds, although mixed-phase clouds play as important roles as warm clouds in the
 1444 evolution of climate and its change. This study provides preliminary mechanisms which
 1445 differentiate mixed-phase clouds and their interactions with aerosols from their warm-
 1446 cloud counterparts, and control the variation of the differentiation in different regions as a
 1447 way of improving our understanding of mixed-phase clouds. It should be mentioned that
 1448 the efficient way of developing general parameterizations, which are for climate models
 1449 and consider all of warm, mixed-phase clouds in various regions and their interactions with
 1450 aerosols, can be achieved by just adding those mechanisms to pre-existing
 1451 parameterizations of much-studied warm clouds instead of developing brand new
 1452 parameterizations from the scratch. Hence, although those mechanisms identified in this
 1453 study may not be complete, they can act as a valuable building block that can streamline
 1454 the development of those general parameterizations.

Deleted: that differences in IWP/LWP and the relative importance of the impacts of INP and CCN on IWP and LWP among different systems of stratocumulus clouds can be explained by

Deleted: .

Deleted: This factor

Deleted: those

Deleted: WP

Deleted: WP

Deleted: .

Deleted:

Deleted: of

1466 **Code/Data source and availability**

1467

1468 Our private computer system stores the code/data which are private and used in this study.
 1469 Upon approval from funding sources, the data will be opened to the public. Projects related
 1470 to this paper have not been finished, thus, the sources prevent the data from being open to
 1471 the public currently. However, if information on the data is needed, contact the
 1472 corresponding author Seoung Soo Lee (slee1247@umd.edu).

1473

1474 **Author contributions**

1475 Essential initiative ideas are provided by SSL, CHJ and YJY to start this work. Simulation
 1476 and observation data are analyzed by SSL, CHJ and JU. YZ, JP, MGM and SKS review
 1477 the results and contribute to their improvement. JC provides supports to set up and run
 1478 additional simulations during the review.

1479

1480 **Competing interests**

1481 The authors declare that they have no conflict of interest.

1482

1483 **Acknowledgements**

1484 This study is supported by the National Research Foundation of Korea (NRF) grant funded
 1485 by the Korea government (MSIT) (Nos. NRF2020R1A2C1003215,
 1486 NRF2020R1A2C2011081, NRF2023R1A2C1002367,
 1487 NRF2021M1A5A1065672/KOPRI-PN23011 and 2020R1A2C1013278), and Basic
 1488 Science Research Program through the NRF funded by the Ministry of Education (No.
 1489 2020R1A6A1A03044834).

1490

1491

1492

1493

1494

1495

1496

1497

1498

Deleted: ¶

Deleted: the Korea Meteorological Administration Research and Development Program "Research on Weather Modification and Cloud Physics" under Grant (KMA2018-00224)

1509

1510 **References**

1511

1512 [Ackerman, A., Kirkpatrick, M., Stevens, D., et al.: The impact of humidity above](#)
 1513 [stratiform clouds on indirect aerosol climate forcing, *Science*, 432, 1014–1017,](#)
 1514 <https://doi.org/10.1038/nature03174>, 2004.

1515 Albrecht, B. A.: Aerosols, cloud microphysics, and fractional cloudiness, *Science*, 245,
 1516 1227–1230, 1989.

1517 Bartosiewicz, Y., and Duponcheel, M.: Large eddy simulation: Application to liquid metal
 1518 fluid flow and heat transfer . In: Roelofs, Ferry, *Thermal Hydraulics Aspects of Liquid*
 1519 *Metal Cooled Nuclear Reactors*, Woodhead Publishing, 2018.

1520 Brown, A., Milton, S., Cullen, M., Golding, B., Mitchell, J., and Shelly, A.: Unified
 1521 modeling and prediction of weather and climate: A 25-year journey, *B. Am. Meteorol.*
 1522 *Soc.*, 93, 1865–1877, 2012.

1523 Chen, F., and Dudhia, J.: Coupling an advanced land-surface hydrology model with the
 1524 Penn State-NCAR MM5 modeling system. Part I: Model description and
 1525 implementation, *Mon. Wea. Rev.*, 129, 569–585, 2001.

1526 Choi, Y.-S., Ho, C.-H., Park, C.-E., Storelvmo, T., and Tan, I.: Influence of cloud phase
 1527 composition on climate feedbacks, *J. Geophys. Res.*, 119, 3687–3700,
 1528 doi:10.1002/2013JD020582, 2014.

1529 Choi, Y.-S., Lindzen, R. S., Ho, C.-H., and Kim, J.: Space observations of cold-cloud phase
 1530 change, *Proc. Natl. Acad. Sci. U.S.A.*, 107, 11211–11216, 2010

1531 Chua, X. R., and Ming, Y.: Convective invigoration traced to warm-rain microphysics,
 1532 *Geophys. Res. Lett*, 47, <https://doi.org/10.1029/2020GL089134>, 2020.

1533 Dione, C., Lohou, F., Lothon, M., Adler, B., Babić, K., Kalthoff, N., Pedruzo-Bagazgoitia,
 1534 X., Bezombes, Y., and Gabella, O.: Low-level stratiform clouds and dynamical
 1535 features observed within the southern West African monsoon, *Atmos. Chem. Phys.*,
 1536 19, 8979–8997, <https://doi.org/10.5194/acp-19-8979-2019>, 2019.

1537 [Donovan, D. P., Ice-cloud effective particle size parameterization based on combined lidar,](#)
 1538 [radar reflectivity, and mean Doppler velocity measurements, *J. Geophys. Res.*, 108,](#)
 1539 [4573, doi:10.1029/2003JD003469](#), 2003.

1540 [Donovan, D. P., van Lammeren, A.C.A.P., Hogan, R. J., Russchenberg, H. W. J., Apituley,](#)

Deleted: ¶

Formatted: Font: Not Italic

Formatted: Font: Not Italic

Formatted: Font: Not Bold

- 1543 [A., Francis, P., Testud, J., Pelon, J., Quante, M., and Goddard, J. W. F.: Cloud effective](#)
1544 [particle size and water content profile retrievals using combined lidar and radar](#)
1545 [observations – 2. Comparison with IR radiometer and in situ measurements of ice](#)
1546 [clouds, J. Geophys. Res, 106, 27449-27464, 2001.](#)
- 1547 Dudhia, J., Numerical study of convection observed during the winter monsoon
1548 Experiment using a mesoscale two-dimensional Model, *J. Atmos. Sci.*, 46, 3077–3107,
1549 <https://doi.org/10.1175/1520-0469>, 1989.
- 1550 Fan, J., Rosenfeld, D., Zhang, Y., Giangrande, S. E., Li, Z., Machado, L. A. T., Martin, S.
1551 T., Yang, Y., Wang, J., and Artaxo, P.: Substantial convection and precipitation
1552 enhancements by ultrafine aerosol particles. *Science*, 359, 411–418, 2018
- 1553 Forster, P., et al., Changes in atmospheric constituents and in radiative forcing, in: *Climate*
1554 *change 2007: the physical science basis*, Contribution of working group I to the Fourth
1555 Assessment Report of the Intergovernmental Panel on Climate Change, edited by
1556 Solomon, S., et al., Cambridge Univ. Press, New York, 2007.
- 1557 Hahn, C. J., and Warren, S. G.: A gridded climatology of clouds over land (1971–96) and
1558 ocean (1954–97) from surface observations worldwide, Numeric Data Package NDP-
1559 026EORNL/CDIAC-153, CDIAC, Department of Energy, Oak Ridge, TN, 2007.
- 1560 Hannak, L., Knippertz, P., Fink, A. H., Kniffka, A., and Pante, G.: Why do global climate
1561 models struggle to represent low-level clouds in the West African summer monsoon?,
1562 *J. Climate*, 30, 1665–1687, <https://doi.org/10.1175/JCLI-D-16-0451.1>, 2017
- 1563 Hartmann, D. L., Ockert-Bell, M. E., and Michelsen, M. L.: The effect of cloud type on
1564 earth’s energy balance—Global analysis, *J. Climate*, 5, 1281–1304, 1992.
- 1565 Hartmann, M., Gong, X., Kecorius, S., van Pinxteren, M., Vogl, T., Welti, A., Wex, H.,
1566 Zeppenfeld, S., Herrmann, H., Wiedensohler, A., and Stratmann, F.: Terrestrial or
1567 marine – indications towards the origin of ice-nucleating particles during melt season
1568 in the European Arctic up to 83.7° N, *Atmos. Chem. Phys.*, 21, 11613–11636,
1569 <https://doi.org/10.5194/acp-21-11613-2021>, 2021.
- 1570 [Hogan, R. J., Illingworth, A. J., O’Connor, E. J., et al.: Cloudnet: Evaluation of model](#)
1571 [clouds using ground-based observations, ECMWF Workshop on parametrization of](#)
1572 [clouds on large-scale models., 2006.](#)
- 1573 IPCC: *Climate Change: The Physical Science Basis*. Contribution of Working Group I to

- 1574 the Sixth Assessment Report of the Intergovernmental Panel on Climate Change
1575 [Masson-Delmotte, V., Zhai, P., Pirani, A., Connors, S. L., Péan, C., Berger, S., Caud,
1576 N., Chen, Y., Goldfarb, L., Gomis, M. I., Huang, M., Leitzell, K., Lonnoy, E.,
1577 Matthews, J. B. R., Maycock, T. K., Waterfield, T., Yelekçi, O., Yu, R., and Zhou, B.
1578 (eds.)]. Cambridge University Press, Cambridge, United Kingdom and New York, NY,
1579 USA, In press, doi:10.1017/9781009157896, 2021.
- 1580 Jung, C. H., Yoon, Y. J., Kang, H. J., Gim, Y., Lee, B. Y., Ström, J., Krejci, R., and Tunved,
1581 P.: The seasonal characteristics of cloud condensation nuclei (CCN) in the arctic lower
1582 troposphere, *Tellus B: Chemical and Physical Meteorology*, 70:1, 1513291, [https://doi:
1583 10.1080/16000889.2018.1513291](https://doi:10.1080/16000889.2018.1513291), 2018.
- 1584 Khain, A. P., Ovchinnikov, M., Pinsky, M., Pokrovsky, A. and Krugliak, H.: Notes on the
1585 state-of-the-art numerical modeling of cloud microphysics, *Atmos. Res.*, 55, 159–224,
1586 2000.
- 1587 Khain, A., Pokrovsky, A., Rosenfeld, D., Blahak, U., and Ryzhkov, A.: The role of CCN in
1588 precipitation and hail in a mid-latitude storm as seen in simulations using a spectral
1589 (bin) microphysics model in a 2D dynamic frame, *Atmos. Res.*, 99, 129–146, 2011.
- 1590 Khain, A. P., Phillips, V., Benmoshe, N., Pokrovsky, A.: The role of small soluble aerosols
1591 in the microphysics of deep maritime clouds, *J. Atmos. Sci.*, 69, 2787–2807, 2012.
- 1592 Knippertz, P., Fink, A. H., Schuster, R., Trentmann, J., Schrage, J. M., and Yorke, C.: Ultra-
1593 low clouds over the southern West African monsoon region, *Geophys. Res. Lett.*, 38,
1594 L21808, <https://doi.org/10.1029/2011GL049278>, 2011.
- 1595 Kogan, Y., 2013: A cumulus cloud microphysics parameterization for cloud-resolving
1596 models, *J. Atmos. Sci.*, 70, 1423–1436, <https://doi:10.1175/JAS-D-12-0183.1>, 2013.
- 1597 Koop, T., Luo, B. P., Tsias, A., and Peter, T.: Water activity as the determinant for
1598 homogeneous ice nucleation in aqueous solutions, *Nature*, 406, 611–614.
- 1599 Lee, H., and Baik, J.-J.: A physically based autoconversion parameterization, *J. Atmos. Sci.*,
1600 74, 1599–1616, <https://doi.org/10.1175/JAS-D-16-0207.1>, 2017.
- 1601 Lee S. S., Penner, J. E., and Saleeby, S. M.: Aerosol effects on liquid-water path of thin
1602 stratocumulus clouds, *J. Geophys. Res.*, 114, D07204, doi:10.1029/2008JD010513,
1603 2009.
- 1604 Lee, S. S., et al., Mid-latitude mixed-phase stratocumulus clouds and their interactions with

- 1605 aerosols: how ice processes affect microphysical, dynamic and thermodynamic
1606 development in those clouds and interactions?, *Atmos. Chem. Phys.*,
1607 <https://doi.org/10.5194/acp-21-16843-2021>, 2022.
- 1608 Li, J., Carlson, B. E., Yung, Y. L., Lv, D., Hansen, J., Penner, J. E., Liao, H., Ramaswamy,
1609 V., Kahn, R. A., Zhang, P., Dubovik, O., Ding, A., Lacis, A. A., Zhang, L., and Dong,
1610 Y.: Scattering and absorbing aerosols in the climate system, *Nature Reviews Earth and*
1611 *Environment*, 3, 363–379, <https://doi.org/10.1038/s43017-022-00296-7>, 2022.
- 1612 Lilly, D. K.: The representation of small scale turbulence in numerical simulation
1613 experiments, *Proc. Ibm Sci. Comput. Symp. Environ. Sci.*, 320–1951, 195–210, 1967.
- 1614 Lim, K.-S. S., and Hong, S.-Y.: Development of an effective double-moment cloud
1615 microphysics scheme with prognostic cloud condensation nuclei (CCN) for weather
1616 and climate models, *Mon. Wea. Rev.*, 138, 1587–1612,
1617 doi:10.1175/2009MWR2968.1., 2010.
- 1618 Liu, Y., and Daum, P. H.: Parameterization of the autoconversion. Part I: Analytical
1619 formulation of the Kessler-type parameterizations, *J. Atmos. Sci.*, 61, 1539–1548,
1620 doi:10.1175/1520-0469(2004)061,1539:POTAPI.2.0.CO;2, 2004.
- 1621 Lohmann, U. and Diehl, K.: Sensitivity studies of the importance of dust ice nuclei for
1622 the indirect aerosol effect on stratiform mixed-phase clouds, *J. Atmos. Sci.*, 63, 968-
1623 982, 2006.
- 1624 Mansell, E. R., Ziegler, C. L. and Bruning, E. C., Simulated electrification of a small
1625 thunderstorm with two-moment bulk microphysics, *J. Atmos. Sci.*, 67, 171–194,
1626 doi:10.1175/2009JAS2965.1., 2010.
- 1627 Ming, Y., and Chua, X. R.: Convective invigoration traced to warm-rain microphysics,
1628 *Geophys. Res. Lett.*, 47, doi.org/10.1029/2020GL089134, 2020.
- 1629 Mlawer, E. J., Taubman, S. J., Brown, P. D., Iacono, M. J., and Clough, S. A.: RRTM, a
1630 validated correlated-k model for the longwave, *J. Geophys. Res.*, 102, 16663-1668,
1631 1997.
- 1632 Möhler, O., et al, Efficiency of the deposition mode ice nucleation on mineral dustparticles,
1633 *Atmos. Chem. Phys.*, 6, 3007-3021, 2006.
- 1634 Ovchinnikov, M., Korolev, A., and Fan, J.: Effects of ice number concentration on
1635 dynamics of a shallow mixed-phase stratiform cloud, *J. Geophys. Res.*, 116, D00T06,

- 1636 doi:10.1029/2011JD015888, 2011.
- 1637 Possner, A., Ekman, A. M. L., and Lohmann, U.: Cloud response and feedback processes
 1638 in stratiform mixed-phase clouds perturbed by ship exhaust, *Geophys. Res. Lett.*, 44,
 1639 1964–1972, <https://doi.org/10.1002/2016GL071358>, 2017.
- 1640 Pruppacher, H. R. and Klett, J. D.: Microphysics of clouds and precipitation, 714pp, D.
 1641 Reidel, 1978.
- 1642 Ramaswamy, V., et al.: Radiative forcing of climate change, in *Climate Change 2001: The*
 1643 *Scientific Basis*, edited by J. T. Houghton et al., 349-416, Cambridge Univ. Press,
 1644 New York, 2001.
- 1645 Solomon, A., de Boer, G., Creamean, J. M., McComiskey, A., Shupe, M. D., Maahn, M.,
 1646 and Cox, C.: The relative impact of cloud condensation nuclei and ice nucleating
 1647 particle concentrations on phase partitioning in Arctic mixed-phase stratocumulus
 1648 clouds, *Atmos. Chem. Phys.*, 18, 17047–17059, [https://doi.org/10.5194/acp-18-](https://doi.org/10.5194/acp-18-17047-2018)
 1649 17047-2018, 2018.
- 1650 Smagorinsky, J.: General circulation experiments with the primitive equations, *Mon. Wea.*
 1651 *Rev.*, 91, 99–164, 1963.
- 1652 Stevens, B., and Feingold, G.: Untangling aerosol effects on clouds and precipitation in a
 1653 buffered system, *Nature*, 461, 607–613, <https://doi.org/10.1038/nature08281>, 2009.
- 1654 Stephens, G. L., and Greenwald, T. J.: Observations of the Earth’s radiation budget in
 1655 relation to atmospheric hydrology. Part II: Cloud effects and cloud feedback, *J.*
 1656 *Geophys. Res.*, 96, 15 325–15 340, 1991.
- 1657 Tinel, C., Testud, J., Hogan, R. J., Protat, A., Delanoe, J. and Bouniol, D.: The retrieval of
 1658 ice cloud properties from cloud radar and lidar synergy, *J. Appl. Meteorol.*, 44, 860-
 1659 875, 2005.
- 1660 Tunved, P., Ström, J. and Krejci, R.: Arctic aerosol life cycle: linking aerosol size
 1661 distributions observed between 2000 and 2010 with air mass transport and
 1662 precipitation at Zeppelin station, Ny-Ålesund, Svalbard, *Atmos. Chem. Phys.*,
 1663 13, 3643–3660, <https://doi.org/10.5194/acp-13-3643-2013>, 2013
- 1664 Twomey, S.: Pollution and the Planetary Albedo, *Atmos. Env.*, 8,1251-1256, 1974.
- 1665 Warren, S. G., Hahn, C. J., London, J., Chervin, R. M., and Jenne, R. L.: Global distribution
 1666 of total cloud cover and cloud types over land, NCAR Tech. Note NCAR/TN-

Formatted: Font: (Default) Times New Roman, (Asian) Malgun Gothic, 12 pt, Font color: Black, Pattern: Clear

Formatted: Indent: Left: 0", Hanging: 2 ch

Formatted: Font: (Default) Times New Roman, (Asian) Malgun Gothic, 12 pt, Font color: Black, Pattern: Clear

1667 273+STR, National Center for Atmospheric Research, Boulder, CO, 29 pp. + 200
1668 maps, 1986.

1669 Wood, R.: Stratocumulus clouds, Mon. Wea. Rev., 140, 2373-2423, 2012.

1670 Zhang, D., Vogelmann, A., Kollias, P., Luke, E., Yang, F., Lubin, D., and Wang, Z.:
1671 Comparison of Antarctic and Arctic single-layer stratiform mixed-phase cloud
1672 properties using ground-based remote sensing measurements, J. Geophys. Res., 124,
1673 10186–10204, <https://doi.org/10.1029/2019JD030673>, 2019.

1674 Zheng, Y., Zhang, H., Rosenfeld, D., Lee, S. S., Su, T., and Li, Z.: Idealized Large-Eddy
1675 Simulations of Stratocumulus Advecting over Cold Water. Part I: Boundary Layer
1676 Decoupling, 78, 4089-4102, <https://doi.org/10.1175/JAS-D-21-0108.1>, 2021.

1677
1678
1679
1680
1681
1682
1683
1684
1685
1686
1687
1688
1689
1690
1691
1692
1693
1694
1695
1696
1697
1698
1699
1700
1701
1702
1703
1704
1705
1706
1707

Formatted: Font: (Asian) Malgun Gothic, 12 pt, Font color: Black, (Asian) Korean

Formatted: Font: (Asian) Malgun Gothic, 12 pt, Font color: Black, (Asian) Korean

Formatted: Font: (Asian) Malgun Gothic, 12 pt, Font color: Black, (Asian) Korean

Formatted: Font: (Asian) Malgun Gothic, 12 pt, Font color: Black, (Asian) Korean

Formatted: Font: (Asian) Malgun Gothic, 12 pt, Font color: Black, (Asian) Korean

Formatted: Indent: Left: 0", Hanging: 2 ch

Formatted: Font: (Asian) Malgun Gothic, 12 pt, Font color: Black, (Asian) Korean

Formatted: Font: (Asian) Malgun Gothic, 12 pt, Font color: Black, (Asian) Korean

Formatted: Font: (Asian) Malgun Gothic, 12 pt, Font color: Black, (Asian) Korean

Formatted: Font: (Asian) Malgun Gothic, 12 pt, Font color: Black, (Asian) Korean

Formatted: Font: (Asian) Malgun Gothic, 12 pt, Font color: Black, (Asian) Korean

Formatted: Font: (Asian) Malgun Gothic, 12 pt, Font color: Black, (Asian) Korean

Formatted: Font: (Asian) Malgun Gothic, 12 pt, Font color: Black, (Asian) Korean

Formatted: Font: (Asian) Malgun Gothic, 12 pt, Font color: Black, (Asian) Korean

Formatted: Hyperlink, Font: (Asian) Malgun Gothic, 12 pt, (Asian) Korean

Field Code Changed

1708 **FIGURE CAPTIONS**

1709

1710 Figure 1. A red rectangle marks the simulation domain in the Svalbard area, Norway. The
1711 light blue represents the ocean and the green the land area.

1712

1713 Figure 2. (a) The vertical distributions of the domain-averaged potential temperature and
1714 humidity at the first time step, (b) the time series of the domain-averaged large-scale
1715 subsidence or downdraft at the model top and (c) the time series of the domain-averaged
1716 surface temperature. ▾

1717

1718 Figure 3. Aerosol size distribution at the surface. N represents aerosol number
1719 concentration per unit volume of air and D represents aerosol diameter.

1720

1721 Figure 4. The vertical distributions of the time- and domain-averaged IWC and LWC in
1722 the 200_2 and 200_2_noice runs.

1723

1724 Figure 5. The vertical distributions of the time- and domain-averaged deposition and
1725 condensation rates in the 200_2 and 200_2_noice runs.

1726

1727 Figure 6. The vertical distributions of the time- and domain-averaged IWC and LWC in
1728 the 200_2, 200_2_noice and 200_2_fac10 runs.

1729

1730 Figure 7. The vertical distributions of the time- and domain-averaged (a) IWC in the 200_2,
1731 2000_20, 200_2_fac10, 200_20, 2000_2, 200_2_fac10_CCN10, and 200_2_fac10_INP10
1732 runs. (b) The vertical distributions of the time- and domain-averaged LWC in the
1733 200_2_noice and 2000_2_noice runs as well as all the runs shown in panel (a). ▾

1734

1735

1736

1737

1738 ▾

Deleted: .

Deleted: and (b) LWC

Deleted: .

Deleted: ¶

¶

Simulations	The number concentration of aerosols acting as CCN at the first time step in the PBL (cm^{-3})	The number concentration of aerosols acting as INP at the first time step in the PBL (cm^{-3})	ICNCavg/CDNCavg	Ice processes
200 2	200	2	0.220	Present
2000 20	2000	20	0.201	Present
2000 2	2000	2	0.108	Present
200 20	200	20	0.512	Present
200 2 noice	200	2	0.000	Absent
2000 2 noice	2000	2	0.000	Absent
200 2 fac10	200	0.07	0.022	Present
200 2 fac10 CCN10	2000	0.07	0.012	Present
200 2 fac10 INP10	200	0.7	0.041	Present
200 2 norad	200	2	0.218	Present
2000 2 norad	2000	20	0.197	Present
2000 2 noice norad	2000	2	0.101	Present
200 20 norad	200	20	0.502	Present
200 2 noice norad	200	2	0.000	Absent
2000 2 noice norad	2000	2	0.000	Absent
200 2 fac10 norad	200	0.07	0.022	Present
200 2 fac10 CCN10 norad	2000	0.07	0.010	Present
200 2 fac10 INP10 norad	200	0.7	0.038	Present
4000 45	4000	45	0.220	Present
13 0.1	13	0.1	0.220	Present
4000 1.8 fac10	4000	1.8	0.022	Present
12 0.0035 fac10	12	0.0035	0.022	Present

Formatted: Font: 11 pt
Formatted Table

Formatted: Font: 11 pt

Formatted: Font: 11 pt

Formatted: Font: 11 pt

Formatted: Font: 11 pt

Formatted: Font: 11 pt

Formatted: Font: 11 pt

Formatted: Font: 11 pt

Formatted: Font: 11 pt

Formatted: Font: 11 pt

Formatted: Font: 11 pt

Formatted: Font: 11 pt

Formatted: Font: 11 pt

Formatted: Font: 11 pt

Formatted: Font: 11 pt

Formatted: Font: 11 pt

Formatted: Font: 11 pt

Formatted: Font: 11 pt

Formatted: Font: 11 pt

Formatted: Font: 11 pt

Formatted: Font: 11 pt

Formatted: Font: 11 pt

Formatted: Font: 11 pt

Deleted: ¶

Deleted: ¶

¶

¶

¶

¶

¶

¶

¶

¶

¶

¶

¶

¶

¶

¶

¶

¶

1745

1746 Table 1. Summary of simulations

1747

1748

1749

1750

1751

1752

1753

1754

1755

1756

Simulations	IWC (10^{-3} g m^{-3})	LWC (10^{-3} g m^{-3})	IWP (g m^{-2})	LWP (g m^{-2})	IWC/LWC	IWP/LWP	Condensation rate		Deposition rate		Cloud-base sedimentation ($10^{-3} \text{g m}^{-2} \text{s}^{-1}$)		Entrainment (cm s^{-1})
							Over grid points (10^{-2} g m^{-3} s^{-1})	Over cloudy columns (g m^{-2} s^{-1})	Over grid points (10^{-2} g m^{-3} s^{-1})	Over cloudy columns (g m^{-2} s^{-1})	Ice- crystal	Droplet	
200_2	6.57	0.25	31.94	1.23	26.28	25.96	0.11	1.98	1.30	23.40	1.17	0.17	0.25
2000_20	7.82	0.21	40.91	1.08	37.24	37.91	0.09	1.62	1.57	28.26	0.94	0.06	0.53
2000_2	6.55	0.29	31.85	1.46	22.58	21.81	0.12	2.16	1.28	23.04	1.11	0.08	0.28
200_20	7.80	0.20	40.82	1.01	39.00	40.42	0.09	1.62	1.56	28.08	0.97	0.11	0.51
200_2_noise	0.00	2.06	0.00	10.35	0.00	0.00	0.72	12.48	0.00	0.00	0.00	0.36	0.08
2000_2_noise	0.00	2.25	0.00	11.29	0.00	0.00	0.76	12.80	0.00	0.00	0.00	0.14	0.10
200_2_fac10	0.89	0.85	4.27	4.20	1.05	1.02	0.32	5.76	0.35	6.30	0.19	0.28	0.06
200_2_fac10_CCN10	0.79	0.97	3.82	4.83	0.81	0.79	0.38	6.84	0.31	5.58	0.17	0.19	0.07
200_2_fac10_INP10	0.98	0.78	4.73	3.88	1.25	1.22	0.31	5.58	0.39	7.02	0.14	0.22	0.07

1766

1767 Table 2. The averaged IWC, LWC, IWP, LWP, condensation and deposition rates over all
1768 of grid points and the simulation period in each of simulations. IWC/LWC (IWP/LWP) is
1769 the averaged IWC (IWP) over the averaged LWC (LWP). Also, as shown are the vertically
1770 integrated condensation and deposition rates over each cloudy column which are averaged
1771 over those columns and the simulation period. The average cloud-base sedimentation rate,
1772 which is for each of ice crystals and droplets, over the cloud base and simulation period,
1773 and the average cloud-top entrainment rate over the cloud top and simulation period are
1774 shown as well.

1775

1776

1777

1778

1779

1780

1781

1782

1783

1784

1785

1786

1787

1788

Deleted: 1

Simulations	IWC (10 ⁻³ g m ⁻³)	LWC (10 ⁻³ g m ⁻³)	IWP (g m ⁻²)	LWP (g m ⁻²)	IWC/LWC	IWP/LWP	Condensation rate		Deposition rate		Ice-crystal Droplet Cloud-based sedimentation (10 ⁻³ g m ⁻² s ⁻¹)	
							Over grid points (10 ⁻³ g m ⁻² s ⁻¹)	Over cloudy columns (g m ⁻² s ⁻¹)	Over grid points (10 ⁻³ g m ⁻² s ⁻¹)	Over cloudy columns (g m ⁻² s ⁻¹)		
							200 2 norad	6.42	0.24	31.21		1.22
2000 20 norad	7.63	0.21	40.05	1.07	36.33	37.43	0.09	1.59	1.55	29.91	0.92	0.06
2000 2 norad	6.40	0.29	31.11	1.45	22.06	21.45	0.11	2.12	1.26	22.69	1.07	0.08
200 20 norad	7.61	0.20	39.95	0.99	38.05	40.35	0.09	1.59	1.54	27.72	0.97	0.11
200 2 noice norad	0.00	2.03	0.00	10.20	0.00	0.00	0.72	12.31	0.00	0.00	0.00	0.34
2000 2 noice norad	0.00	2.21	0.00	11.12	0.00	0.00	0.75	12.63	0.00	0.00	0.00	0.13
200 2 fac10 norad	0.87	0.84	4.21	4.17	1.04	1.01	0.31	5.74	0.35	6.21	0.18	0.27
200 2 fac10 CCN10 norad	0.78	0.96	3.78	4.80	0.81	0.79	0.36	6.81	0.30	5.50	0.16	0.18
200 2 fac10 INP10 norad	0.97	0.76	4.70	3.85	1.25	1.22	0.30	5.55	0.38	6.91	0.13	0.21

Table 3. Same as Table 2 but for the repeated simulations with radiative processes turned off.

- Formatted ... [9]
- Formatted ... [10]
- Formatted ... [11]
- Formatted ... [12]
- Formatted ... [13]
- Formatted ... [14]
- Formatted ... [15]
- Formatted ... [16]
- Formatted ... [17]
- Formatted ... [18]
- Formatted ... [19]
- Formatted ... [20]
- Formatted ... [21]
- Formatted ... [22]
- Formatted ... [23]
- Formatted ... [24]
- Formatted ... [25]
- Formatted ... [26]
- Formatted ... [27]
- Formatted ... [28]
- Formatted ... [29]
- Formatted ... [30]
- Formatted ... [31]
- Formatted ... [32]
- Formatted ... [33]
- Formatted ... [34]
- Formatted ... [35]
- Formatted ... [36]
- Formatted ... [37]
- Formatted ... [38]
- Formatted ... [39]
- Formatted ... [40]
- Formatted ... [41]
- Formatted ... [42]
- Formatted ... [43]
- Formatted ... [44]
- Formatted ... [45]
- Formatted ... [46]
- Formatted ... [47]
- Formatted ... [48]
- Formatted ... [49]
- Formatted ... [50]
- Formatted ... [51]
- Formatted ... [52]
- Formatted ... [53]
- Formatted ... [54]
- Formatted ... [55]
- Formatted ... [56]
- Formatted ... [57]
- Formatted ... [58]
- Formatted ... [59]
- Formatted ... [60]
- Formatted ... [61]
- Formatted ... [62]
- Formatted ... [63]
- Formatted ... [64]
- Formatted ... [65]
- Formatted ... [66]
- Formatted ... [67]
- Formatted ... [68]
- Formatted ... [69]

1790
1791
1792
1793
1794
1795
1796
1797
1798
1799
1800
1801
1802
1803
1804
1805
1806
1807
1808
1809
1810
1811
1812

Simulations	ICNCavg/CDNCavg	Percentage increases (+) or decrease (-) in ICNCavg/CDNCavg	IWC/LWC	Percentage increases (+) or decrease (-) in IWC/LWC
200 2 fac10 CCN10	0.012		0.81	
200 2 fac10	0.022	+83.33%	1.05	+29.6%
200 2 fac10 INP10	0.041	+86.36%	1.25	+19.0%
2000 2	0.108	+163.4%	22.58	+1706.4%
2000 20	0.201	+86.1%	37.24	+64.9%
200 2	0.220	+9.4%	26.28	-29.4%
200 20	0.512	+132.7%	39.00	+48.4%

- Formatted: Font: (Asian) Times New Roman, 10 pt
- Formatted: Font: (Asian) Times New Roman, 10 pt
- Formatted: Font: (Asian) Times New Roman, 10 pt
- Formatted: Normal, Centered, None, Line spacing: single
- Formatted Table
- Formatted: Font: (Asian) Times New Roman, 10 pt
- Formatted: Font: (Asian) Times New Roman, 10 pt
- Formatted: Font: 10 pt
- Formatted: Font: (Asian) Times New Roman, 10 pt
- Formatted: Normal, Centered, None, Line spacing: single
- Formatted: Font: 10 pt
- Formatted: Font: (Asian) Times New Roman, 10 pt
- Formatted: Font: (Asian) Times New Roman, 10 pt
- Formatted: Normal, Centered, None, Line spacing: single
- Formatted: Font: (Asian) Times New Roman, 10 pt
- Formatted: Normal, Centered, None, Line spacing: single
- Formatted: Font: (Asian) Times New Roman, 10 pt
- Formatted: Font: (Asian) Times New Roman, 10 pt
- Formatted: Font: (Asian) Times New Roman, 10 pt
- Formatted: Font: (Asian) Times New Roman, 10 pt
- Formatted: Normal, Centered, None, Line spacing: single
- Formatted: Font: (Asian) Times New Roman, 10 pt
- Formatted: Font: (Asian) Times New Roman, 10 pt
- Formatted: Font: (Asian) Times New Roman, 10 pt
- Formatted: Normal, Centered, None, Line spacing: single
- Formatted: Font: (Asian) Times New Roman, 10 pt
- Formatted: Font: (Asian) Times New Roman, 10 pt
- Formatted: Font: (Asian) Times New Roman, 10 pt
- Formatted: Normal, Centered, None, Line spacing: single
- Formatted: Font: (Asian) Times New Roman, 10 pt
- Formatted: Font: (Asian) Times New Roman, 10 pt
- Formatted: Superscript
- Deleted: ¶

1817
1818
1819
1820
1821
1822
1823
1824
1825
1826
1827
1828
1829
1830
1831
1832
1833
1834
1835
1836
1837
1838
1839
1840

Table 4. ICNCavg/CDNCavg and IWC/LWC in the simulations that are related to Section 4.1. The Percentage increases or decreases in ICNCavg/CDNCavg and IWC/LWC in the j^{th} row are $\frac{(ICNCavg/CDNCavg)_{i+1} - (ICNCavg/CDNCavg)_i}{(ICNCavg/CDNCavg)_i} \times 100 (\%)$ and $\frac{(IWC/LWC)_{i+1} - (IWC/LWC)_i}{(IWC/LWC)_i} \times 100 (\%)$, respectively. Here, $(ICNCavg/CDNCavg)_i$ and $(IWC/LWC)_i$ represent ICNCavg/CDNCavg and IWC/LWC in the i^{th} row, respectively.

<u>Simulations</u>	<u>ICNCavg/CDNCavg</u>	<u>IWC/LWC</u>	<u>Percentage increases (+) or decrease (-) in IWC/LWC</u>
<u>Polar case</u>			
<u>200_2</u>	<u>0.220</u>	<u>26.28</u>	
<u>4000_45</u>	<u>0.220</u>	<u>27.25</u>	<u>+3.7%</u>
<u>13_0.1</u>	<u>0.220</u>	<u>25.62</u>	<u>-2.5%</u>
<u>Representing midlatitude case</u>			
<u>200_2_fac10</u>	<u>0.022</u>	<u>1.05</u>	
<u>4000_1.8_fac10</u>	<u>0.022</u>	<u>1.09</u>	<u>+3.8%</u>
<u>12_0.0035_fac10</u>	<u>0.022</u>	<u>1.02</u>	<u>-2.9%</u>

Formatted: Font: (Default) Batang, (Asian) Batang

Formatted: Left

1842

1843 Table 5. ICNCavg/CDNCavg and IWC/LWC in the simulations that are related to Section1844 4.2. The percentage increases or decreases in IWC/LWC in the 4000_45 run or in the1845 13_0.1 run are $\frac{(IWC/LWC)_{4000_45 \text{ or } 13_0.1} - (IWC/LWC)_{200_2}}{(IWC/LWC)_{200_2}} \times 100 (\%)$. Here,1846 $(IWC/LWC)_{4000_45 \text{ or } 13_01}$ represents IWC/LWC in the 4000_45 run or the 13_01 run, while1847 $(IWC/LWC)_{200_2}$ represents IWC/LWC in the 200_2 run. The percentage increases or1848 decreases in IWC/LWC in the 4000_1.8_fac10 run or the 12_0.0035_fac10 run are1849 $\frac{(IWC/LWC)_{4000_1.8_fac10 \text{ or } 12_0.0035_fac10} - (IWC/LWC)_{200_2_fac10}}{(IWC/LWC)_{200_2_fac10}} \times 100 (\%)$. Here,1850 $(IWC/LWC)_{4000_1.8_fac10 \text{ or } 12_0.0035_fac10}$ represents IWC/LWC in the 4000_1.8_fac10 run or1851 the 12_0.0035_fac10 run, while $(IWC/LWC)_{200_2_fac10}$ represents IWC/LWC in the1852 200_2_fac10 run.

1853

1854

1855

1856

1857

1858

1859

1860

1861

1862

1863

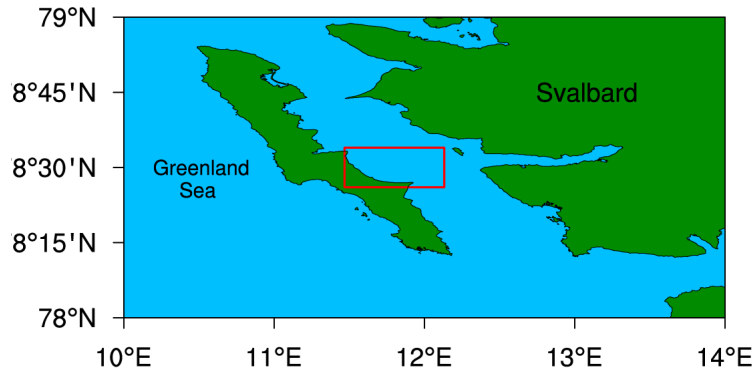
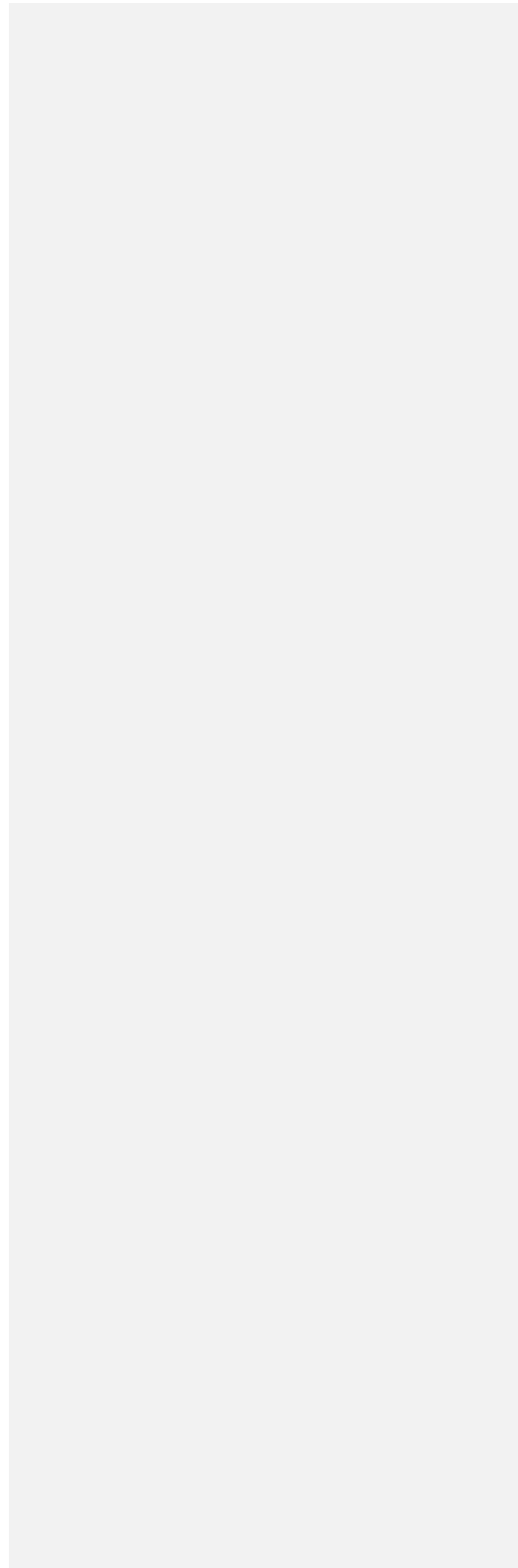


Figure 1

1864
1865
1866
1867
1868
1869
1870
1871
1872
1873
1874
1875
1876
1877
1878
1879
1880
1881
1882
1883



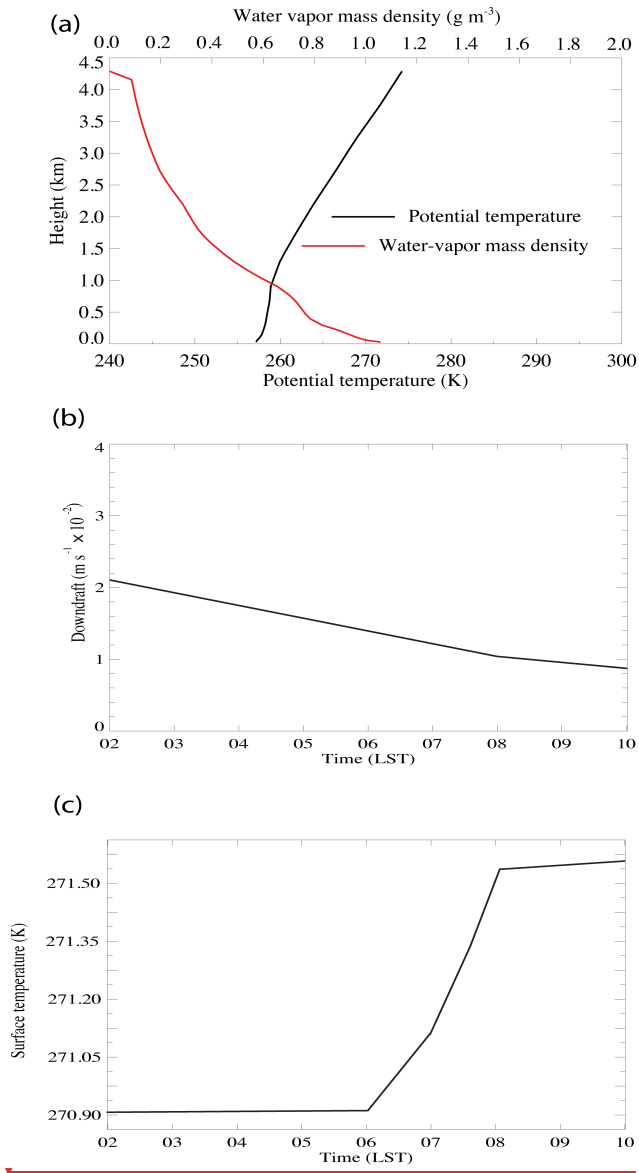
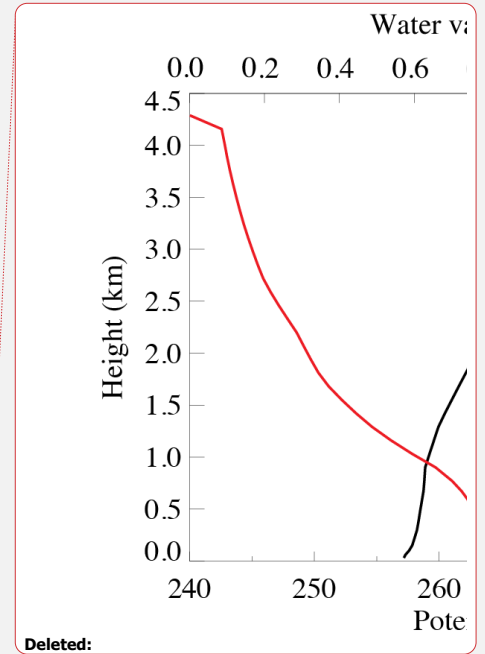


Figure 2



Deleted:

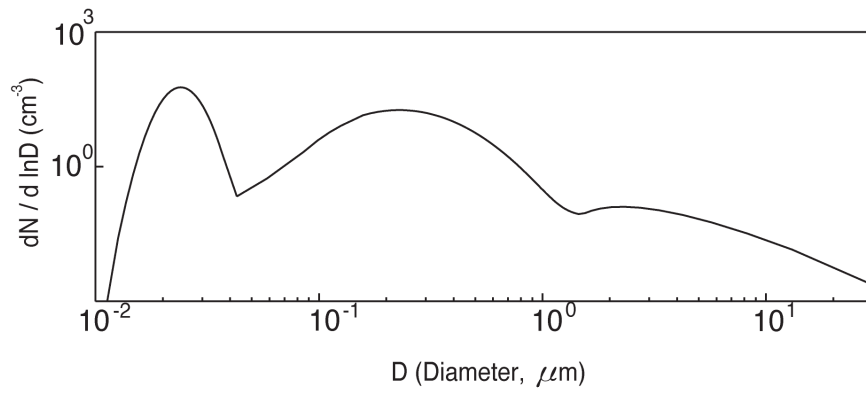
Deleted:

Deleted:



1884

1885

**Figure 3**

1895

1896

1897

1898

1899

1900

1901

1902

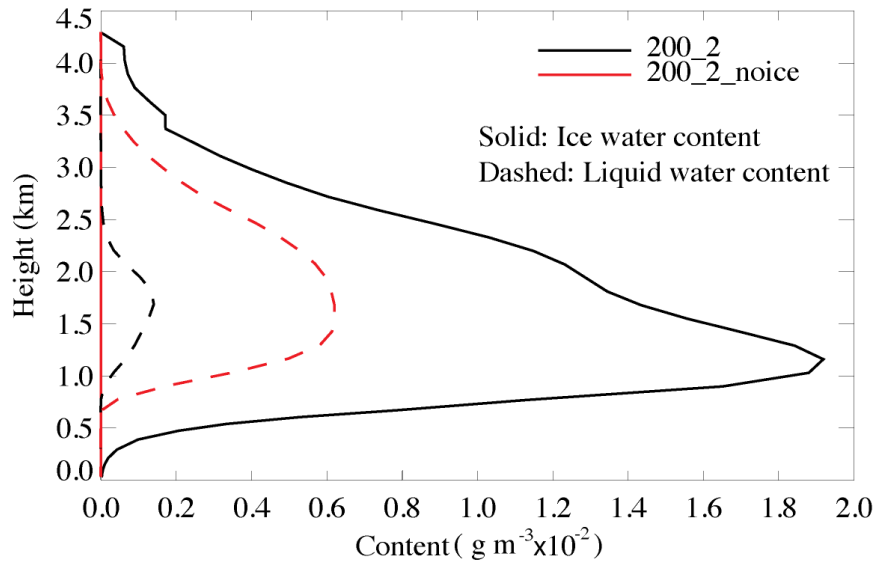
1903

1904

1905

1906

1907

**Figure 4**

1908

1909

1910

1911

1912

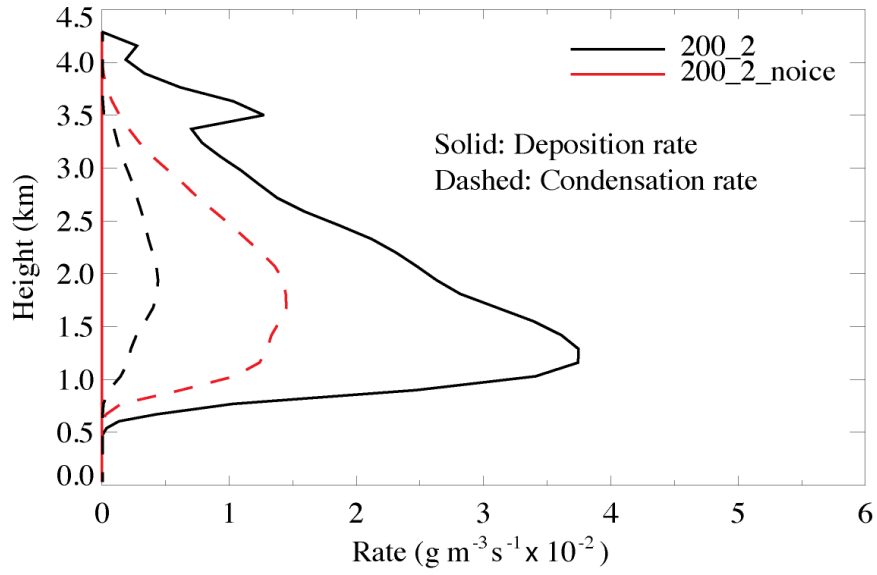
1913

1914

1915

1916

1917

**Figure 5**

1918

1919

1920

1921

1922

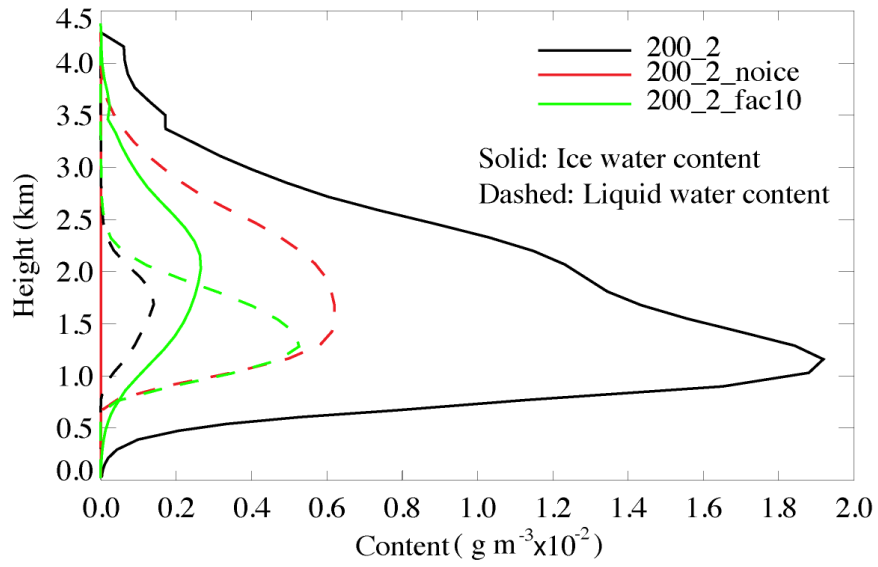
1923

1924

1925

1926

1927

**Figure 6**

1928

1929

1930

1931

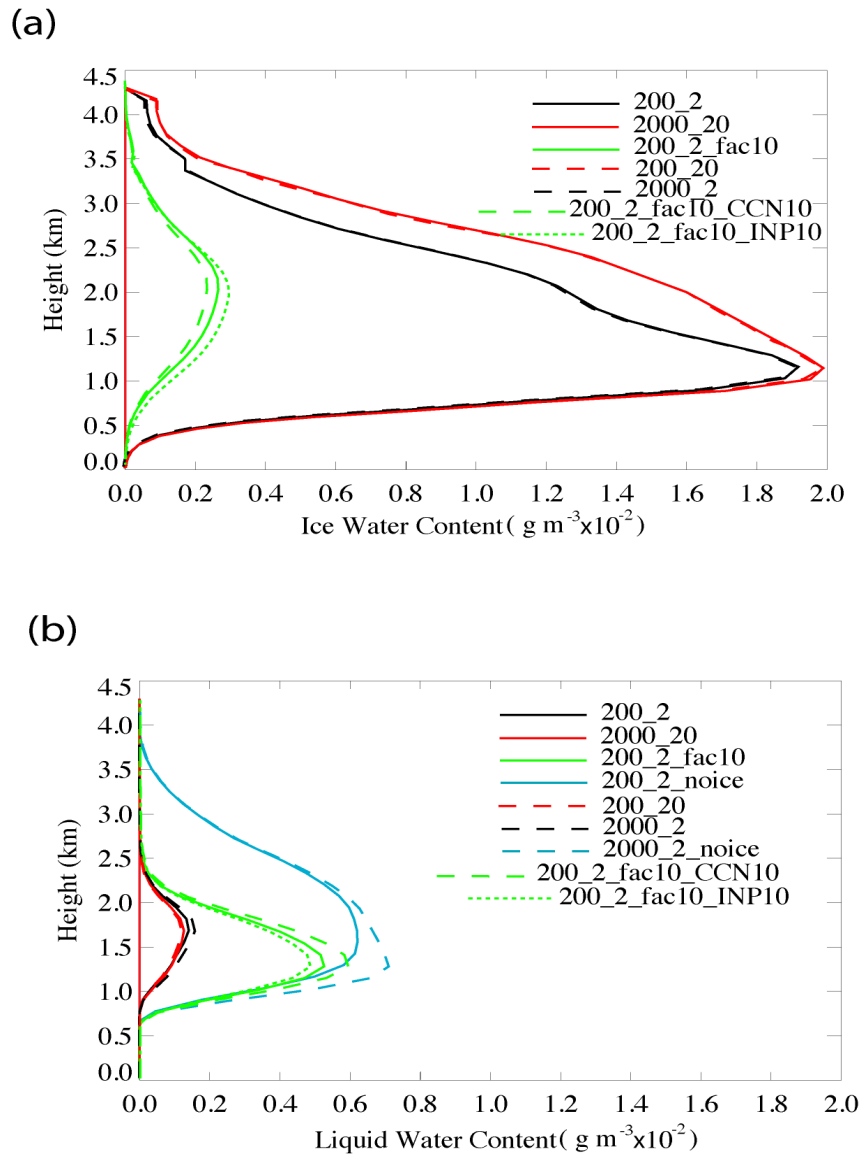
1932

1933

1934

1935

1936



1937

1938

Figure 7